Testing the gravitational interaction in the field of the Earth via Satellite Laser Ranging and the LAser RAnged Satellites Experiment (LARASE)

D M Lucchesi[a,b,c], L Anselmo[b], M Bassan[d,c], C Pardini[b], R Peron[a,c], G Pucacco[d,c] and M Visco[a,c]

[a] Istituto di Astrofisica e Planetologia Spaziali (IAPS/INAF), Via del Fosso del Cavaliere 100, 00133 Roma, Italy

[b] Istituto di Scienza e Tecnologie della Informazione (ISTI/CNR), Via G. Moruzzi 1, 56124 Pisa, Italy

[c] Istituto Nazionale di Fisica Nucleare (INFN), Sezione di Roma Tor Vergata, Via della Ricerca Scientifica 1, 00133 Roma, Italy

[d] Dipartimento di Fisica, Università di Roma Tor Vergata, Via della Ricerca Scientifica 1, 00133 Roma, Italy

E-mail: david.lucchesi@iaps.inaf.it

Abstract.

In this work the LAser RAnged Satellites Experiment (LARASE) is presented. This is a research program that aims to perform new refined tests and measurements of gravitation in the field of the Earth in the weak field and slow motion (WFSM) limit of general relativity (GR). For this objective we use the free available data relative to geodetic passive satellites laser tracked from a network of ground stations by means of the Satellite Laser Ranging (SLR) technique.

After a brief introduction to GR and its WFSM limit, which aims to contextualize the physical background of the tests and measurements that LARASE will carry out, we focus on the current limits of validation of GR and on current constraints on the alternative theories of gravity that have been obtained with the precise SLR measurements of the two LAGEOS satellites performed so far. Afterward we present the scientific goals of LARASE in terms of upcoming measurements and tests of relativistic physics.

Finally, we introduce our activities and we give a number of new results regarding the improvements to the modelling of both gravitational and non-gravitational perturbations to the orbit of the satellites. These activities are a needed prerequisite to improve the forthcoming new measurements of gravitation. An innovation with respect to the past is the specialization of the models to the LARES satellite, especially for what concerns the modelling of its spin evolution, the neutral drag perturbation and the impact of Earth's solid tides on the satellite orbit.

Keywords: General Relativity, Artificial satellites, Satellite Laser Ranging, Gravitational and Non–gravitational Perturbations, Tides Submitted to: *Class. Quantum Grav.*

1. Introduction

Einstein's theory of general relativity (GR) represents the best theory we have at our disposal for the description of the gravitational interaction (Einstein 1916), both at the high and low energy scales, and it is the pillar of modern cosmology to understand the universe that we observe through a number of different techniques. Indeed, after 100 years, GR has passed a wide number of experimental verifications (Will 1993, Will 2014) and it is currently considered the "Standard Model" for gravitational physics.

Einstein's GR is a geometric theory of gravity (*geometrodynamics*) — where gravity is a manifestation of spacetime curvature — and is fully described by the metric tensor $g_{\mu\nu}$. Therefore, Einstein's GR is a metric theory for the description of the gravitational interaction.

Besides GR, other metric theories of gravitation have been developed during the years (Jordan 1949, Brans & Dicke 1961, Dicke 1962, Dicke 1964, Dicke 1968, Ni 1973, Rosen 1973, Rosen 1978), just to cite a few of them. Metric theories of gravitation share with Einstein's *geometrodynamics* the same spacetime structure and the same equations of motion for test particles, but differ in the field equations form. Moreover, metric theories are the only theories for the gravitational interaction that fully embody the Einstein Equivalence Principle (EEP), which relies on the Weak Equivalence Principle (WEP) and represents its generalization to all the laws of special relativity.

Indeed, Einstein's theory is founded on a hypothesis that produces a unique property for gravity, i.e., that the gravitational force (in Newtonian words) is composition independent or, equivalently, in a gravitational field all bodies — regardless of being macroscopic or microscopic in their essence and/or in the way they interact and independently of their mass and composition — fall with the same acceleration.

This hypothesis arises from the universality of free fall (UFF) of Galilei and Newton: the acceleration imparted to a body by a gravitational field is independent of the nature of the body. If this is true, inertial and gravitational mass are equivalent, following Newton. This is the WEP, and Newton made this "principle of equivalence" the basis of his mechanics. Einstein extended this principle to the invariance of physical laws in a (non-rotating) laboratory freely falling in a uniform gravitational field (Einstein 1908, Schwartz 1977), and making it at the foundation — as a postulate — of his GR. EEP is composed, in the modern view, of three fundamental pieces: i) weak equivalence principle (WEP), ii) local lorentz invariance (LLI), and iii) local position invariance (LPI). This composition suggests three possible (and different) ways to test EEP from the experimental point of view. See e.g. (Will 1993) for the chosen terminology.

Metric theories different from general relativity provide additional fields (scalar, vectorial, tensorial) beside the metric tensor $g_{\mu\nu}$, that act as "new" gravitational fields. The role of these fields is to "explain" how the matter and the non-gravitational fields generate the gravitational fields themselves and produce the metric. Instead, as previously underlined, GR is mediated by just one tensor field and has an exact

symmetry given by EEP.

Therefore, during the last fifty years it has been of great importance to test GR — in all its many facets — versus other metric and also non–metric theories of gravitation to gain the best interpretation of the gravitational interaction. This has been possible thanks to the development of new technologies, such as that of the atomic clocks, the beginning of the space era, with radar and laser ranging, and also thanks to a number of fundamental discoveries in the field of astrophysics and cosmology, such as quasars, cosmic background radiation, pulsars and black holes, see (Schmidt 1963, Penzias & Wilson 1965, Hewish et al. 1968) and (Kerr 1963, Wheeler 1964, Penrose 1965, Bolton 1972).

However, in addition to the many theoretical and experimental triumphs of GR, several open points are still present: i) the theory predicts spacetime singularities (Penrose 1965), but is not able to explain them (quantum physics may come to play an important role to explain these breaking points of the theory, see also below in the text); ii) the emission of gravitational radiation, which is predicted by Einstein's theory, was observed only indirectly in its effect on the orbit of a binary system of two neutron stars (Hulse & Taylor 1975, Kramer et al. 2006), but it has never been observed directly as a twist of spacetime by a gravitational bar detector (Astone et al. 2010) or by an interferometer (Adhikari 2014, Bizouard 2014); iii) apparently, about 95% of the observed universe seems constituted by a mass–energy content that the theory is not able to explain (Riess et al. 1998, Bennett et al. 2003, Ruhl et al. 2003). Therefore, from all these considerations it is clear the importance to verify the predictions of GR with respect to the other proposed theories.

Moreover, the possible existence of additional fields in mediating the gravitational interaction is not only predicted by other (alternative) theories of gravitation, but also by modern theories of physics which aim to unify gravity with the quantum realm. Indeed, one more fundamental aspect is connected with the fact that Einsten's GR is a classical (i.e., non-quantum) theory of physics. Indeed, all the attempts at merging gravitation with the other three interactions of nature, in order to encompass all physics in a New Standard Model, have failed.

In the framework of a unified quantum field theory, the Standard Model (SM) provides an interesting and well-tested description of the electromagnetic interaction with the nuclear (weak and strong) interactions. Therefore, there are fundamental theoretical motivations in order to extend the current SM in such a way to include, at the Planck scale, the (generally) very weak gravitational interaction into a quantum scenario with the other fundamental interactions of nature. These extensions of the SM, as for instance string theory (Veneziano 1968) or the more complete M-theory (Witten 1995), must of course reduce to Einstein's theory of general relativity in the appropriate limit and, in particular, to Newtonian gravity in their non-relativistic limit. It is important to stress that the SM has twenty free parameters that have been adjusted through the experimental results while, in the case of string theory, we have no free parameters to adjust experimentally.

These theories predict new physical effects that are "suitable" for experimental investigation. In fact, one of the main characteristics of such theories is that they contain (new) light-bosons which produce (new) weak forces, i.e., the existence of further fields to be considered from the theoretical point of view and to be measured from the experimental one. Anyway, it is important to stress that currently none of the predictions of these theories has been verified from the experimental point of view.

However, as we have seen above, the alternative theories for gravity (all classical and non-quantum), as well as the just cited quantum theories, provide scalar and/or vector fields in mediating the gravitational interaction in addition to the metric tensor of GR. This represents a natural bridge between modern theories of physics (also those arising from particle physics) and all other theories for the gravitational interaction that are different from Einstein's *geometrodynamics*.

Such additional interactions are generally responsible of violations of the WEP (see e.g. (Damour & Polyakov 1994, Damour 1996)). Therefore, violations of the WEP, if measured, are the signature of the presence of additional very weak non-gravitational forces related with the exchange of light-bosons which couple to ordinary (baryonic) matter with a strength not much different from gravity. Currently, the best tests of the WEP through the UFF — at the level of 10^{-13} — have been obtained in the field of the Earth (Schlamminger et al. 2008) and in the field of the Sun (Baeßler et al. 1999) with torsion balance experiments, as well as via Lunar Laser Ranging (LLR) experiments in the field of the Sun (Williams et al. 2012). Space tests of the WEP aim to go a step further with respect to current results, with a goal of about 10^{-15} in the case of μScope (Touboul et al. 2012) and a goal of about 10^{-17} in the case of GG (Nobili et al. 2012).

However, such possible violations may be investigated also through the propagation of the electromagnetic waves (Shapiro 1990, Bertotti et al. 2003) or via their impact on the very long-term behaviour of the orbital parameters of a binary system, as in the case of the argument of pericenter (Nordtvedt 1998, Nordtvedt 2000, Lucchesi & Peron 2010, Lucchesi & Peron 2014).

It is precisely in this context — characterized by a wide and intricate theoretical background, from geometrodynamics until metric and non-metric theories of gravity up to modern quantum physics theories with deep implications at different scales — that the new research program we are proposing, denominated LAser RAnged Satellites Experiment (LARASE), aims to provide an original contribution in testing and verifying relativistic physics by means of the powerful Satellite Laser Ranging (SLR) technique together with a precise orbit determination (POD) of a dedicated set of passive laser-ranged satellites.

It is worth mentioning that this background of theories is also quite difficult to test clearly in a reliable manner, because of the non-linearity of the gravitational interaction, in order to definitely distinguish one possible contribution from another. A special role is played by the reliability of the final error budget, in terms of the contribution of the systematic effects, with the analysis of the possible effects of aliasing.

By means of a POD it is possible to solve for a number of *a priori* unknown

parameters (in principle) that reflect the impact of the relativistic effects on the orbit of the considered satellites and, at the same time, it is possible to provide a reliable estimate of the (possible) correlations among the relativistic parameters and all the other significant ones that enter the dynamical model used to describe the satellites orbit. All these aspects represent important prerequisites for the construction of an estimate of the systematic errors — in the case of new measures of relativistic effects — that must be robust and accurate.

The paper is organised as follows. In section 2, the weak-field and slow-motion limit of general relativity will be briefly recalled with its main characteristics. In section 3, the state of the art in testing Einstein's theory of general relativity in the field of the Earth by means of SLR will be highlighted. In section 4, the objectives of LARASE, in terms of the relativistic effects to be measured and of the main disturbing effects that need to be better modelled, will be described. In section 5, we will introduce our approach to the orbit determination problem, with the description of the dynamical models used as well as our preliminary results. In section 6, we will focus on the activities that we started in order to improve the current models of the main non–gravitational perturbations as well as of the tidal effects. Finally, in section 7, our conclusions and recommendations will be highlighted with the activities to be performed in the near future.

2. The weak-field and slow-motion limit of general relativity

Scientists, as well as philosophers, are well aware that no theory is fully correct, and any new theory represents, from the epistemological point of view, a completion of a previous one with a deeper insight into the laws of nature and a better comprehension of previous "*known*" physical phenomena. Indeed a new theory, if not falsified, can be widely considered, or at least accepted, as "*truth*". Therefore, in the definition of an experiment to be done to analyze a given phenomenon of nature, we need at the same time to fix the rules of the theory we want to falsify under the considered experiment.

In the framework of the "*experimental*" activities we are going to perform with LARASE, we are not (directly) interested in GR as the background theory to put under investigation and falsify, but to a simplified and linearized version of the full theory which is valid in the weak-field and slow-motion limit of Einstein's theory.

This approach leads to the post-Newtonian (PN) approximation, see below. However, and very interestingly, the PN approximation results very efficient also in describing the regime of strong fields and fast motion when it is expanded at high orders (Will 2011). These considerations reinforce the importance of all efforts aiming to test gravity in the weak-field and slow-motion limit of GR, as those we are trying to pursue with LARASE.

2.1. The WFSM limit of GR

As briefly highlighted in the previous Introduction, Einstein's general relativity is a geometric theory of gravity, where gravity is a manifestation of spacetime curvature, and it is fully described by the metric tensor $g_{\mu\nu}$, a symmetric and non-degenerate tensor (Einstein 1916). In particular, once defined a curved manifold with a metric — more precisely a 4-dimensional pseudo-Riemannian manifold — it is possible to define the infinitesimal length interval ds:

$$ds^2 = c^2 d\tau^2 = g_{\mu\nu} dx^\mu dx^\nu, \tag{1}$$

where c represents the speed of light, constant and invariant, $d\tau$ is the infinitesimal proper time, and x^μ represents an arbitrary coordinate system.

The essential point is that, in Einstein's GR, the length interval ds between any two (infinitesimally) close events of the spacetime (such as x^μ and $x^\mu + dx^\mu$) remains invariant under any general change of coordinates.

This is the principle of *general covariance* of GR. This principle further states that all physical equations must retain their form, i.e., are to be *covariant*, under a general coordinate transformation: $x^\mu \to x'^\mu$. Therefore, the metric tensor needs to be also covariant. This is spacetime general covariance, indeed a revolutionary concept. Newton's laws, as well as those of special relativity hold only in inertial frames, hence are not generally covariant.

The full theory of GR leads to Einstein's field equations:

$$G_{\mu\nu} = 8\pi \frac{G}{c^4} T_{\mu\nu}, \tag{2}$$

where $G_{\mu\nu}$ represents Einstein's tensor (it is built from the metric tensor and from its first and second derivatives), $T_{\mu\nu}$ represents the stress–energy tensor (a zero divergence and frame-independent tensor which acts as a source of gravity), finally G represents the gravitational constant. Because $T_{\mu\nu}$ has null divergence, $G_{\mu\nu}$ is conserved.

According to Einstein's equations, mass–energy (described by the stress–energy tensor) *tells* geometry (described by the metric tensor) how to *curve*, and the geometry — from Einstein's equations — *tells* mass–energy how to *move*. This is a very important aspect, and a way in order to discriminate, from the experimental point of view, between GR and other metric theories of the gravitational interaction.

As we have remarked, metric theories of gravitation share with GR the same spacetime structure (i.e., the same pseudo-Riemannian character) and the same equations of motion for test particles, but differ in the field equations form. In other words, in metric theories different from GR:

- the spacetime geometry *tells* mass–energy how to *move* as in GR;
- but mass–energy *tells* spacetime geometry how to *curve* in a different way from GR;
- and the metric alone acts back on the mass in agreement with EEP.

We refer to Chapter 3 of (Ciufolini & Wheeler 1995) as well as to (Will 1993) for a deeper insight into the relationships between GR and other metric theories, as well as the relationships between metric (and non-metric) theories and Einstein's equivalence principle.

Unfortunately, despite the beauty and simplicity of the ideas that led Einstein to the development of this revolutionary theory for the gravitational interaction, the field equations are very complicated to be solved, and we are able to solve them analytically only in a few special cases characterized by particular symmetries, such as the spherical one.

Luckily, there is a significant number of very interesting physical situations in which approximations to the solutions of the equations are sufficient. In fact, Einstein's field equations may be written in a very simple way if we consider the so-called weak-field and slow-motion (WFSM) limit of GR. This linear approximation of Einstein theory can be applied in the case of the Earth: in fact, we deal with a source (the Earth) whose gravitational field is weak ($GM_\oplus/R_\oplus \ll 1$) and whose rotation is not relativistic (where $M_\oplus$ and $R_\oplus$ represent, respectively, Earth's mass and radius).

Indeed, given the relative smallness of the masses at play (that of the Earth as well as that of the artificial satellites), as well as that of their speed when compared with that of light ($v \ll c$), the WFSM formulation of the theory is sufficient for our purpose.

Einstein's equations are partial differential equations of the second order in the metric tensor $g_{\mu\nu}$ of spacetime. In the WFSM limit of the theory, these equations reduce to a form quite similar to those of electromagnetism.

Under these approximations, the metric tensor of the curved spacetime may be re–written in terms of that of flat spacetime, i.e., of the Minkowskian metric tensor $\eta_{\mu\nu}$, plus small corrections that are related to the curvature produced by masses as well as by mass currents:

$$g_{\mu\nu} \simeq \eta_{\mu\nu} + h_{\mu\nu}. \tag{3}$$

In this equation, the quantities $h_{\mu\nu}$ represent the deviations from the flat spacetime of special relativity and are such that $|h_{\mu\nu}| \ll 1$, at least in the Solar System and in agreement with the WFSM limit.

Following this approach we have a gravitoelectric field produced by masses, analogous to the electric field produced by charges, and a gravitomagnetic field produced by mass currents, analogous to the magnetic field produced by electric currents.

These two fields, respectively $\mathbf{E}_{\rm GE}$ and $\mathbf{B}_{\rm GM}$, in the WFSM limit of GR can be expressed in terms of a scalar potential Φ and of a vector potential $\mathbf{A}$ (Ciufolini & Wheeler 1995, Mashhoon et al. 2001):

$$\mathbf{E}_{\rm GE} = -\nabla\Phi - \frac{1}{2c}\frac{\partial \mathbf{A}}{\partial t}, \tag{4}$$

$$\mathbf{B}_{\rm GM} = \nabla \times \mathbf{A}, \tag{5}$$

where

$$\Phi \simeq -\frac{GM_\oplus}{r}, \tag{6}$$

which arises from the so-called electric components of the metric, and

$$\mathbf{A} \simeq \frac{2G}{c}\frac{\mathbf{r}\times\mathbf{J}_{\oplus}}{r^3}, \tag{7}$$

which arises from the so-called magnetic components of the metric. In Eq. (7), $\mathbf{r}$ represents the satellite position from the Earth's center of mass, while $\mathbf{J}_{\oplus}$ is the Earth's angular momentum, i.e., its intrinsic spin. Practically, the spin (generated by mass currents) plays the same role played by the magnetic moment (generated by currents) in classical electrodynamics.

The two fields above are responsible for two relativistic precessions on the orbit of a satellite. Indeed, the satellite orbit around the Earth can be considered as a sort of enormous gyroscope subject to the torques produced by the gravitoelectric and gravitomagnetic forces.

These are: the i) Einstein (or Schwarzschild) (Einstein 1916), and ii) Lense-Thirring (LT) (Lense & Thirring 1918, Mashhoon et al. 1984) precessions, using the name of who first discovered each effect. The former precession arises from the gravitoelectric field, while the latter is due to the gravitomagnetic one. These relativistic precessions are responsible for secular effects on two of the three Euler angles that define the orbit orientation in space, namely the argument of pericenter, ω, which is subject to both precessions, and the right ascension of the ascending node, Ω, which is subject to the Lense-Thirring one‡.

In addition to these two precessions, and in the frame of a relativistic three-body problem, where the two primaries are the Sun and the Earth and the test particle is represented by a satellite orbiting the Earth, we have to consider also the de Sitter (or geodetic) precession (de Sitter 1916). This precession is effective on the right ascension of the ascending node and on the orbit inclination i, the last of the three Euler angles, and it arises from the coupling between the Earth-satellite system and the background field of the Sun.

Einstein's (or Schwarzschild's) precession is due to the mass of the primary, it is therefore a spin-independent secular effect. The other precessions are usually interpreted as frame-dragging effects, but with two very important differences:

(i) the Lense-Thirring precession is intrinsically related to the spin of the primary body, i.e., with its rotation, and arises from the additional curvature produced by the rotation of the primary; it is also known as frame-dragging effect;

(ii) conversely, the de Sitter precession is frame-dependent, it arises from the motion of a test-gyroscope (the Earth-satellite system) on the static background of the Sun (i.e., assumed non-rotating).

In other words, while the de Sitter precession can be cancelled by an appropriate change of coordinates — in such a way to null the speed of the test-gyroscope with

‡ It is worth mentioning that the gravitoelectric field is also responsible for a secular effect on the mean anomaly $\mathcal{M}$ of the satellite.

respect to the non-rotating Sun — the Lense-Thirring precession can never be cancelled by any change of coordinates. Therefore, the Lense-Thirring precession must be related to an *intrinsic* gravitomagnetism. We refer to Section 6.11 of (Ciufolini & Wheeler 1995) for a deeper insight into gravitomagnetism and its invariant character.

Following (Huang et al. 1990), a formulation of the relevant equations of motion in a geocentric non-inertial reference system (non-rotating with respect to the solar barycentric one) is possible. This is the formulation implemented in the main codes used for a POD of the orbit of a satellite. It has to be noticed that the problem of a consistent local relativistic formulation of reference frames and equations of motion is not trivial. This problem has been tackled in a series of papers, starting from (Ashby & Bertotti 1984, Ashby & Bertotti 1986). The resulting models are condensed in the IAU 2000 resolutions for astrometry, celestial mechanics and metrology (see (Soffel et al. 2003) and (Damour et al. 1991, Damour et al. 1992, Damour et al. 1993, Damour et al. 1994), to which we refer for a deeper discussion).

In agreement with this formulation, the accelerations responsible for the above relativistic precessions are:

$$\mathbf{a}_{\rm Schw} = \frac{GM_\oplus}{c^2 r^3}\left[\left(\frac{4GM_\oplus}{r} - v^2\right)\mathbf{r} + 4(\mathbf{v}\cdot\mathbf{r})\mathbf{v}\right], \tag{8}$$

which arises from the gravitoelectric curvature of spacetime induced by Earth's mass-energy $M_\oplus$,

$$\mathbf{a}_{\rm LT} = \frac{2GM_\oplus}{c^2 r^3}\left[\frac{3}{r^2}(\mathbf{r}\times\mathbf{v})(\mathbf{r}\cdot\mathbf{J}_\oplus) + \mathbf{v}\times\mathbf{J}_\oplus\right], \tag{9}$$

which arises from the gravitomagnetic curvature of spacetime induced by Earth's mass-energy currents $\mathbf{J}_\oplus$,

$$\mathbf{a}_{\rm dS} = 2\boldsymbol{\Omega}_{dS}\times\mathbf{v}, \tag{10}$$

which arises from the Earth-satellite motion in the spacetime curved by the Sun mass-energy $M_\odot$, where

$$\boldsymbol{\Omega}_{\rm dS} \approx -\frac{3}{2}(\mathbf{V}_\oplus - \mathbf{V}_\odot)\times\frac{GM_\odot\mathbf{X}_{\oplus\odot}}{c^2 R^3_{\oplus\odot}} \tag{11}$$

represents the de Sitter precession.

In the notation we follow in general (Ashby & Bertotti 1986, Huang et al. 1990), where small letters refer to the geocentric reference frame and capital letters to the solar barycentric one. In particular, $\mathbf{r}$ and $\mathbf{v}$ are the test mass position and velocity in the geocentric frame, $\mathbf{V}_\oplus$ and $\mathbf{V}_\odot$ are the Earth and Sun barycentric velocities, $\mathbf{X}_{\oplus\odot}$ is the Earth-Sun vector, with distance $R_{\oplus\odot}$.

Using the methods of celestial mechanics (see for instance (Soffel 1989)), the effects of the relativistic corrections in the satellite Keplerian elements can be evaluated. In particular, for the three Euler angles that define the orbit orientation in space: ω, Ω and i. Here we focus on the satellite argument of pericenter ω, and on the right ascension of the ascending node Ω. The results for the orbit inclination will be discussed in a forthcoming paper dedicated to the de Sitter effect.

Therefore, following GR, the secular behavior for the pericenter rate is given by

$$\dot{\omega}^{\rm Rel} = \dot{\omega}^{\rm Ein} + \dot{\omega}^{\rm LT}, \tag{12}$$

where

$$\dot{\omega}^{\rm Ein} = \frac{2+2\gamma-\beta}{3}\frac{3(GM_\oplus)^{3/2}}{c^2a^{5/2}(1-e^2)} \tag{13}$$

denotes the gravitoelectric or "*Einstein*" part (Einstein 1915), and

$$\dot{\omega}^{\rm LT} = \frac{1+\gamma}{2}\frac{-6GJ_\oplus}{c^2a^3(1-e^2)^{3/2}}\cos i \tag{14}$$

the gravitomagnetic or "*Lense-Thirring*" part (Lense & Thirring 1918), respectively.

Conversely, in the case of the right ascension of the ascending node for its secular behavior we have:

$$\dot{\Omega}^{\rm Rel} = \dot{\Omega}^{\rm LT} + \dot{\Omega}^{\rm dS}, \tag{15}$$

where

$$\dot{\Omega}^{\rm LT} = \frac{1+\gamma}{2}\frac{2GJ_\oplus}{c^2a^3(1-e^2)^{3/2}} \tag{16}$$

denotes the gravito-magnetic or "*Lense-Thirring*" part (Lense & Thirring 1918), and

$$\dot{\Omega}^{\rm dS} = \left(\frac{1}{2}+\gamma\right)\frac{GM_\odot}{c^2R^3_{\oplus\odot}}|(\mathbf{V}_\oplus-\mathbf{V}_\odot)\times\mathbf{X}_{\oplus\odot}|\cos\epsilon_\odot \tag{17}$$

the geodetic or "*de Sitter*" part (de Sitter 1916), respectively. In the last equation, $\epsilon_\odot \simeq 23.45^\circ$ represents the obliquity of the Earth's orbit with respect to its equatorial plane. Obviously, the geodetic effect is the same for every satellite in orbit around the Earth.

In the previous equations, the GR precessions have been expressed as a function of the parameterized post-Newtonian (PPN) parameters β and γ, see (Nordtvedt 1968, Will 1971, Will & Nordtvedt 1972, Nordtvedt & Will 1972). These are two among the ten parameters that are necessary to describe the post-Newtonian limit in the so-called standard post-Newtonian gauge, see e.g. Chapter 4.2 of (Will 1993) (and also (Poisson & Will 2014)) for details.

In Einstein's theory, all PPN parameters are zero with the exception of γ and β, both equal to unity: γ measures the space curvature per unit of mass, while β describes, in the standard post–Newtonian gauge, the non-linearity of the gravitational interaction in the time component of the metric tensor:

$$g_{00} = -1 - 2\frac{\Phi}{c^2} - 2\beta\frac{\Phi^2}{c^4} + \ldots, \tag{18}$$

where the dots stand for the contribution of additional post-Newtonian potentials and of the other PPN parameters in the case of metric theories different from GR: $\xi, \alpha_1, \alpha_2, \alpha_3, \zeta_1, \zeta_2, \zeta_3, \zeta_4$.

In a forthcoming paper, we will focus on the impact of these additional PPN parameters on the ideal two–body orbit of a satellite around the Earth. As a matter of fact, the investigation on these parameters may help us in discriminating on the possibility of possible preferred-location effects (ξ), or possible preferred-frame effects ($\alpha_1, \alpha_2, \alpha_3$) and, finally, on the possible violation of the total momentum conservation ($\zeta_1, \zeta_2, \zeta_3, \zeta_4$).

Indeed, as we briefly described in the Introduction and at the beginning of this section, in GR and in other metric theories, the metric tensor represents the only gravitational field that enters the equations of motion. However, the other (possible) gravitational fields that other metric theories suggest may help in generating additional spacetime curvature, i.e., they may contribute to the metric together with the matter, but they cannot interact (directly) with matter.

This is sufficient in explaining the importance of the PPN formalism in order to test the validity of metric theories at the post–Newtonian order. At the same time, it is also important to stress that the ten PPN parameters may not be sufficient to test every possible conceivable metric theory for the gravitational interaction at the post–Newtonian order; see Section 3.7 of (Ciufolini & Wheeler 1995) for details.

Under this point of view, and also as a consequence of previous discussion about frame-dependent gravitomagnetism versus intrinsic gravitomagnetism, it should be preferable to express the Lense-Thirring precessions of Eqs. (14) and (16) not as a function of the PPN parameter γ, but as a function of a different parameter μ, i.e., replace $(1+\gamma)/2$ with μ:

$$\dot{\omega}^{\rm LT} = \mu \frac{-6GJ_\oplus}{c^2 a^3 (1-e^2)^{3/2}} \cos i, \tag{19}$$

$$\dot{\Omega}^{\rm LT} = \mu \frac{2GJ_\oplus}{c^2 a^3 (1-e^2)^{3/2}}. \tag{20}$$

In this perspective, and in agreement with the discussion of Sections 3.4.3 and 6.11 of (Ciufolini & Wheeler 1995), μ should not be considered a standard PPN parameter, nor it is a function of one (or more) of them. In other words, in terms of metric $g_{\mu\nu}$, μ measures the contribution to the metric of the spacetime curvature that arises from mass–energy currents relative to other masses.

The reader interested in the mathematical details for the derivation of the above equations for the secular rates may refer to (Will 1993, Ciufolini & Wheeler 1995, Poisson & Will 2014), as well as to the classical textbooks of (Weinberg 1972) and (Misner et al. 1973). Conversely, for an alternative derivation of the Lense-Thirring effect, we also refer to (Chashchina et al. 2009).

3. SLR contribution to GR measurements: state of the art

The Satellite Laser Ranging (SLR) technique represents a powerful and impressive tracking system that allows recovery of the two-way time of flight of laser pulses from

a ground station to cube corner retro-reflectors (CCRs) on a satellite (for a valuable discussion of this technique see e.g. (Degnan 1985)). The observable is represented by the round-trip time of short laser pulses measured by means of very precise time devices down to a resolution of about 10 ps or less (1 ps $= 1 \cdot 10^{-12}$ s). The station-satellite distance (range) is obtained after an averaging procedure over a short time period (bin) that depends both on the structure and height of the satellite. The ranges obtained after the averaging procedure are called Normal Points (NPs), see (Sinclair 1997). These high quality data are presently gathered by the International Laser Ranging Service (ILRS), with range NPs characterized by a mm precision in their root-mean-square (RMS), see (Pearlman et al. 2002).

In the case of the two LAGEOS satellites (see Figure 1), currently the best tracked satellites around the Earth, the cited mm precision in the RMS of their NPs corresponds to an accuracy in the orbit reconstruction at a few cm level, when using the best dynamical models in their data reduction as well as empirical accelerations (these are usually applied in order to account for unmodeled effects, see Section 5).

Therefore, from these considerations it is obvious the key role played by this technique in the case of precise relativistic measurements in the field of Earth. In fact, the size of the general relativistic effects is dictated by the value of the Schwarzschild radius of the primary body around which the satellite is in free fall along its *geodesic*, once removed the perturbing effects due to the non-gravitational forces. In the case of the Earth, for the Schwarzschild radius we obtain:

$$R_{\rm Sch} = 2\frac{GM_{\oplus}}{c^2} \simeq 1\text{cm} \tag{21}$$

which is of the same order of magnitude of the level of accuracy reached by the SLR technique.

A second important aspect is played by the accuracy of the dynamical models implemented in the software used for the data reduction. Indeed, their quality directly impacts the final POD reached by the analysis of the satellite's orbit.

The goal of the software code is to minimize, in a least-squares fit sense, an appropriate function (also known as *cost*-function) and solve for the unknowns we are interested in. Indeed, these models have to account for both gravitational and non-gravitational forces in such a way to reduce as much as possible the difference between the *observed* range and the *computed* (from the models) one.

The better the minimization process through the orbit data reduction from one side and the better the estimate of the systematic error sources from the other, the more precise and accurate will be the *a posteriori* reconstruction of the satellite orbit. Indeed, concerning the estimation problem, the orbit determination is reduced to the least-squares solution of the so-called range residuals:

$$O_i - C_i = -\sum_j \frac{\partial C_i}{\partial P_j} dP_j + dO_i \tag{22}$$

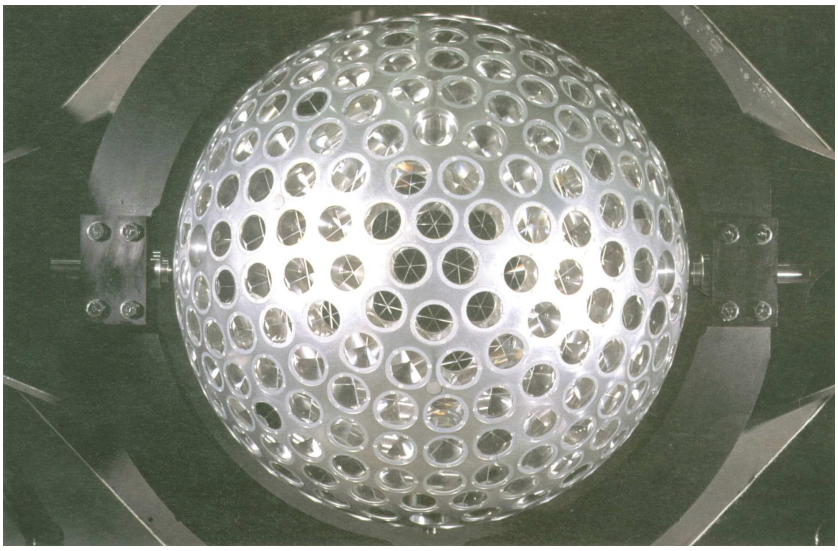

Figure 1. Picture of the LAGEOS II satellite (courtesy of ASI). Launched by ASI/NASA space agencies at the end of October 1992, LAGEOS II is one of the best tracked satellites all over the word by the SLR technique. LAGEOS II is almost a twin of the older LAGEOS (NASA, 1976), see Section 6. Spherical in shape (their radius is only 30 cm), passive (i.e., with no solar panels, instruments, engines or antennae for radio communications with the ground), the external aluminum surface of these geodetic satellites is covered with 426 CCRs for satellite laser ranging. In the case of LAGEOS II, the satellite direct orbit has an inclination of about 53° over the Earth's equator, a semi-major axis of about 12,163 km (corresponding to an orbital period of about 13,348 s) and an orbital eccentricity of about 0.014. The older LAGEOS has an orbit inclination of about 110°, a semi-major axis of about 12,270 km (corresponding to an orbital period of about 13,526 s) and an orbital eccentricity of about 0.004. The smaller inclination of LAGEOS II has been chosen to obtain a better visibility from the network of the Earth laser ranging stations. The satellite area-to-mass ratio of these satellites is quite small in order to minimize the impact of the non-gravitational perturbations (NGPs). See Section 4 for further details.

where O_i and C_i are, respectively, the SLR range observations and their computed (from the dynamical models) values, dP_j represent the corrections to the vector $\mathbf{P}$ of parameters to be estimated and, finally, dO_i are the errors associated with each observation. With regard to the errors dO_i, they account for both the contribution from the noise in the observations as well as for the incompleteness of the mathematical model included in the software used for the orbit determination.

Therefore, it is of extreme importance to have at the same time good observations and good models in order to perform the measurements of the tiny relativistic effects predicted by Einstein's theory, and to verify these predictions with respect to those of other proposed (alternative) theories of the gravitational interaction.

3.1. The Lense-Thirring effect measurements

The first measurements of the relativistic effects with the SLR technique start only after 1995 when, in addition to the good laser observations of the two LAGEOS provided by the ILRS, the systematic errors of the dynamical models — in particular the errors associated with the even zonal harmonics of the Earth's geopotential — became sufficiently small to allow the first detection of the impact of the secular relativistic precession produced by the Lense-Thirring effect on the orbit of the satellites, see (Ciufolini et al. 1996).

The first successful model of the Earth's gravitational field, under this perspectives, was the JGM-3 model jointly developed by the Center for Space Research (CSR) — of the University of Texas at Austin — and by NASA GSFC, see (Tapley et al. 1996).

This first measurement of the Lense-Thirring effect was obtained analyzing the data of the two LAGEOS satellites over a time span of about 2 years and the result was:

$$\mu \simeq (1.3 \pm 0.2) \pm 0.3, \tag{23}$$

where μ represents the normalized general relativistic precession on the combined node of the two LAGEOS satellites and on the argument of pericenter of LAGEOS II ($\mu = 1$ in Einstein's GR and $\mu = 0$ in Newtonian physics), see Section 2.

In the above equation, 0.2 represents the RMS of the final fit to the combined residuals, while 0.3 (i.e., 30%), represents the error budget estimated in (Ciufolini et al. 1996) that arises from the main systematic effects due to both gravitational and non-gravitational perturbations. In equation (23), the quantity 0.3 was also the discrepancy with respect to the prediction of GR, i.e., $\mu = 1.3$ vs. $\mu = 1$. This first estimate of the error budget around 30% has been successively reviewed and increased, see e.g. (Lucchesi 2001).

Indeed, following (Ciufolini 1996), the residuals of these three orbital elements were combined in such a way to cancel out the errors due to the Earth's quadrupole and octupole uncertainties (in fact, the main systematic errors were those associated with the uncertainties of the even zonal harmonics δJ_n of the expansion in spherical harmonics of the gravitational field of the Earth) while solving for the relativistic parameter μ that describes the GR combined precession (about 60.2 mas/yr) that arises from the Lense-Thirring effect (see Eqs. (19) and (20)):

$$\mu \simeq \frac{\delta\dot{\Omega}_{\rm I}^{\rm res} + k_1\delta\dot{\Omega}_{\rm II}^{\rm res} + k_2\delta\dot{\omega}_{\rm II}^{\rm res}}{60.2}, \tag{24}$$

where $\delta\dot{\Omega}_{\rm I}^{\rm res}$, $\delta\dot{\Omega}_{\rm II}^{\rm res}$ and $\delta\dot{\omega}_{\rm II}^{\rm res}$ represent the residuals in the rate of the elements after the data reduction of the orbit of the two satellites (see (Lucchesi & Balmino 2006)), while $k_1 = -0.295$ and $k_2 = +0.350$ are the two coefficients that arise from the solution of a system of three equations in three unknowns. For a further discussion of the combinations concept see also (Peron 2013).

With the term *residual* of an orbital element we mean the unmodeled effects that impact this element after the orbit data reduction of the satellite over a given time span

(arc), 14-day in the case of the two LAGEOS. We refer to Section 5 and to (Lucchesi & Balmino 2006) for further details and for a deeper insight on the meaning of orbital residuals.

A subsequent analysis of the orbit of the two satellites, extended to a period of about 3 years and with the same model JGM-3 for the Earth's gravitational field, provided a new measurement with a fit characterized by a smaller discrepancy with respect to the prediction of GR, but with the same difficulties with regard to the correct estimate of the error budget that arises from the systematic effects of gravitational origin, and of their consequent underestimation, see (Ciufolini, Chieppa, Lucchesi & Vespe 1997) and (Ciufolini, Lucchesi, Vespe & Chieppa 1997):

$$\mu \simeq (1.1 \pm 0.2) \pm 0.3. \tag{25}$$

This procedure for the measurement of the Lense-Thirring effect dates back to 1984, when I. Ciufolini suggested the use of two LAGEOS satellites with supplemenary inclinations in order to cancel out the errors due to the even zonal harmonics of the Earth's geopotential on the combined nodes of the two satellites, see (Ciufolini 1984) and also (Ciufolini 1986, Ciufolini 1989).

Indeed, a big effort was done at that time, with a wide international community involved, and culminated with a proposal to NASA for a third LAGEOS satellite to be launched in supplementary orbital configuration with respect to the older LAGEOS, in the context of the so-called LAGEOS III Experiment, see (Tapley et al. 1989).

In fact, in the case of two satellites in exactly supplementary orbit configuration (i.e., all the orbital elements coincident, but with the sum of their inclination equal to 180°), the relativistic Lense-Thirring precession on their ascending node are equal (i.e., $\dot{\Omega}_{\rm I}^{\rm LT} = \dot{\Omega}_{\rm III}^{\rm LT}$), while the secular precession of the ascending node due to the Earth's deviation from the spherical symmetry are equal and opposite (i.e., $\dot{\Omega}_{\rm I}^{\rm class} = -\dot{\Omega}_{\rm III}^{\rm class}$) as they are both proportional to the cosine of the orbit inclination i:

$$\dot{\Omega}^{\rm class} = -\frac{3}{2} n \left(\frac{R_\oplus}{a}\right)^2 \frac{\cos i}{(1-e^2)^2} \left\{ J_2 + J_4 \left[\frac{5}{8} n \left(\frac{R_\oplus}{a}\right)^2 \left(7\sin^2 i - 4\right) \frac{\left(1+\frac{3}{2}e^2\right)^2}{\left(1-e^2\right)^2} \right] + \dots \right\}, \tag{26}$$

where n represents the satellite mean motion.

For completeness, it is worth mentioning that, in the scientific literature and from the historical point of view of the proposals for the Lense-Thirring effect measurement, it has been H. Yilmaz in 1959, well aware of the perturbing effect of the classical precession provoked by the Earth's oblateness, that proposed to launch a new satellite in a polar orbit in such a way to cancel all these aliasing effects (Yilmaz 1959). Then, about 15 years later, (van Patten & Everitt 1976) proposed to launch two drag-free and counter-orbiting satellites in nearly polar orbits to measure their (combined) Lense-Thirring precession on the two nodes. About two years later, (Cugusi & Proverbio 1978) suggested using the existing laser-ranged satellites, and among them LAGEOS, in order to take advantage of the precise SLR technique to measure the post-Newtonian

corrections of GR to their orbits and, in particular, the Lense-Thirring secular precession of their ascending nodes.

A step forward in the measurement of the Lense–Thirring effect with the two LAGEOS satellites was performed in 1998 with the inclusion of EGM96 in the dynamical models used for the satellites orbit determination. EGM96 represents one of the last multi–satellite models for the gravitational field of the Earth and was jointly developed by NASA/GSFC and NIMA (Lemoine & et al. 1998). In this case the orbit analysis of the two satellites was extended up to four years, and the result was (Ciufolini et al. 1998):

$$\mu \simeq (1.1 \pm 0.03) \pm 0.2. \tag{27}$$

As we can see, this measurement confirmed the previous measure in terms of the discrepancy between the measured precession and that predicted by GR, i.e., a 10% agreement, but with an higher precision in the final fit: 3% with respect to 20%.

However, with regard to the overall accuracy of the measurement, the actual estimate of 20% of the systematic effects was illusory, because of the high correlation among the gravity field coefficients (in particular for the low degree even zonal harmonics to which the two LAGEOS are most sensitive to) despite their smaller formal uncertainties with respect to previous models; see (Ries et al. 2003) for a dedicated discussion.

The problem of a precise and, especially, accurate measurement of the relativistic Lense-Thirring precession on the orbit of the two LAGEOS satellites has found a first significant improvement with the launch of the CHAMP (July, 2000) and GRACE (March, 2002) satellites (see (Reigber et al. 2002, Reigber et al. 2003, Reigber et al. 2005, Tapley & Reigber 2001)).

Both missions use Global Positioning System (GPS) receivers and accelerometer measurements (Touboul et al. 1999) in order to precisely determine their orbits and remove the non–gravitational accelerations from the list of unknowns. These satellites are also equipped with CCRs for SLR measurement of their orbit.

One of the characteristics of the Earth gravity models derived from these missions is to improve the gravity field knowledge with a limited amount of data and, especially, in the medium and long wavelengths regions of its spectrum. A significant consequence has been an overall better accuracy in the determination of the gravity field coefficients as well as a strong reduction of the correlations among the various coefficients, in particular of the even zonal ones to which we are mainly interested in. Unfortunately, because of the low altitude of these satellites (about 500 km at the beginning of their mission), the lower degree coefficients have not been so significantly improved with respect to the accuracy provided by EGM96§.

In this context it is also important to distinguish between formal uncertainties and calibrated ones. The calibration procedures aim to estimate the systematic errors

§ Moreover, the analysis of the orbit of the LAGEOS satellites has strongly contributed to the estimate of their current values and uncertainties.

Table 1. Comparison between EGM96 and EIGEN-GRACE02S formal (for) and calibrated (cal) uncertainties for the first five even zonal harmonics.

Coefficient	EGM96 (for)	EIGEN-GRACE02S (for)	EIGEN-GRACE02S (cal)
$\delta\bar{C}_{2,0}$	0.3561×10^{-10}	0.1433×10^{-11}	0.5304×10^{-10}
$\delta\bar{C}_{4,0}$	0.1042×10^{-9}	0.4207×10^{-12}	0.3921×10^{-11}
$\delta\bar{C}_{6,0}$	0.1450×10^{-9}	0.3037×10^{-12}	0.2049×10^{-11}
$\delta\bar{C}_{8,0}$	0.2266×10^{-9}	0.2558×10^{-12}	0.1479×10^{-11}
$\delta\bar{C}_{10,0}$	0.3089×10^{-9}	0.2347×10^{-12}	0.2101×10^{-11}

that may have impacted the determination of the coefficients of the gravity field model during the POD of the satellite(s) orbit and the subsequent procedures of data analysis. Indeed, the calibration of the coefficients is a very important and complicated issue which is rarely performed with reliability. We refer to Section VIII.A of (Lucchesi & Peron 2014) for a detailed discussion on this topic.

For instance, in the case of the EIGEN-GRACE02S model (Reigber et al. 2005), their formal errors were calibrated with a procedure based on the scattering of subset solutions. In this case, each solution was generated from data covering different periods of the GRACE mission. In particular, the variances per degree of the coefficients differences between the considered subset solutions were compared with the formal error degree variances as resulting from the adjustment. We refer to the literature for further details (Reigber et al. 2005).

In Table 1 are shown the formal uncertainties of the first five even zonal harmonics (for the normalized Stokes coefficients) in the case of the EGM96 and EIGEN-GRACE02S models, compared with the calibrated errors of EIGEN-GRACE02S.

From this table it is clear that the formal errors of EGM96 are much larger than those of EIGEN-GRACE02S (between one and three orders of magnitude), while the calibrated errors of EIGEN-GRACE02S are about a factor of 10 larger than their corresponding formal errors.

One of the great advantages of the higher precision and of the very low correlations among the various coefficients from the new models for the Earth's gravitational field arising from the GRACE mission resides in the possibility of taking out the LAGEOS II satellite argument of pericenter in the combination of equation (24).

Indeed, the argument of pericenter of the two LAGEOS satellites is very sensitive to the perturbation due to the thermal effects, especially to the Yarkovsky–Schach effect provoked by the direct solar radiation pressure, when its absorption is modulated by the satellite eclipses, see Section 6.2. If such perturbation is not modelled, as in the case of the past measurements of the Lense-Thirring effect, unmodelled long-period effects will modify the pericenter evolution, with a subsequent change in the slope of the relativistic precession to be recovered from the combination of the orbital residuals, see (Ciufolini 1996), (Lucchesi 2002) and (Lucchesi et al. 2004). Conversely, the ascending

node of the satellite is less perturbed by the unmodelled Yarkovsky–Schach effect, see (Farinella et al. 1990) and (Lucchesi 2002).

Therefore, in this case, only the two nodes of the LAGEOS satellites were combined in such a way to remove both the static and the time-dependent errors related with the first even zonal harmonic coefficient (J_2) while solving for the relativistic precession:

$$\mu \simeq \frac{\delta\dot{\Omega}_{\rm I}^{\rm res} + k_3\delta\dot{\Omega}_{\rm II}^{\rm res}}{48.2}, \tag{28}$$

where $k_3 \simeq 0.545$, and 48.2 mas/yr represents the GR value of the relativistic precession to be measured. For an explicit derivation of Eq. (28) see (Iorio & Morea 2004).

It is also important to stress that a large fraction of the error associated with the 18.6-year tide is due to the uncertainty δJ_2 in the knowledge of the quadrupole coefficient. This tide, as well as the 9.3-year tide, is due to the so–called Moon nodes line regression. Hence, with the combinations of Eqs. (24) and (28) also these tidal errors are further reduced (cancelled in principle) concerning their impact in the relativistic measurement; see also Section 6.4.

Indeed, in 2004 a new measurement of the Lense-Thirring effect was performed by (Ciufolini & Pavlis 2004) using the EIGEN-GRACE02S model as the background field for the Earth's geopotential and Eq. (28). They obtained:

$$\mu \simeq (0.99 \pm 0.12) \pm 0.05(\pm 0.10). \tag{29}$$

This analysis of the orbit of the two LAGEOS satellites was performed over a time span of about 11 years. The combined residuals of Eq. (28) were fitted — after the removal of six periodic effects — by means of a function composed of a linear term plus phases and amplitudes of six main periodic signals, corresponding to a 13-parameter fit. The authors obtained a linear term of about 47.9 mas/yr, corresponding to a 1% discrepancy with respect to the prediction of GR, with a RMS of their post–fit residuals of about 6 mas, which corresponds to a 12% error in their best fit.

With regard to the error budget estimate, due to possible systematic uncertainties, the authors first estimated a value of about 5% due to the contribution of gravitational and non-gravitational perturbations added together in a root–sum–square fashion. About 80% of this error was originated by the even zonal harmonics with degree $\ell \geq 4$, and largely dominated by the uncertainty in the J_4 coefficient. Finally, considering other possible unknown errors, also related to an underestimate of the even zonal harmonics uncertainties, the authors have considered, conservatively, an overall error budget of about 10%.

This result represents the most accurate measurement of the Lense-Thirring effect performed so far, and it has also been confirmed independently by other teams, also using new (and more recent) models for the Earth's gravitational field (see (Ries & Eanes 2012, Ries et al. 2008, Koenig et al. 2012)).

Still in 2004, a more precise but less accurate measurement of the Lense-Thirring precession was obtained by analysing nine years of the orbits of LAGEOS and of

LAGEOS II with the EIGEN2S gravitational field (Reigber et al. 2003) from the CHAMP mission, see (Lucchesi 2004*b*, Lucchesi 2007). The result was:

$$\mu \simeq (0.99 \pm 0.01) \pm 0.18, \tag{30}$$

with a RMS discrepancy of just 1% with respect to the prediction of GR, obtained with a simple linear fit to the combined and integrated node residuals of the two satellites. The error budget is at 1–σ level, and it is dominated by the uncertainties of the even zonal harmonics with degree $\ell \geq 4$ obtained by the formal (and uncalibrated) errors of the EIGEN2S model, of about 17.8%.

In this work, the fit to the combined residuals of the two satellites was carried out over a nine years time span. This is due to the fact that the oscillations on the combined nodes provoked by the non-gravitational perturbations (NGP) are close to full cycles over this time span. Consequently, the periodic disturbing effects of the NGP on the orbit of the two LAGEOS satellites are smaller, on the average, than those on longer or shorter time spans. In this way, the impact of the unmodelled part of the NGP is strongly reduced both in the fit to the residuals and in the estimate of their (systematic) unmodelled effects, about 0.4%, see (Lucchesi 2007) for details. Indeed, the fit obtained by (Ciufolini et al. 2006) with the EIGEN2S model over a ten years period was characterized by a much larger RMS discrepancy: about 32% when fitting for a linear trend only, and about 11% when fitting for a linear trend plus ten periodic signals. All the data reductions quoted above for a POD of the two LAGEOS satellites for the measurement of the Lense-Thirring effect have been performed with the software GEODYN II of NASA/GSFC, see (Pavlis & et al. 1998).

With regard to the Lense-Thirring effect measurement, it is worth mentioning the NASA and Stanford University space mission denominated Gravity Probe B (GP-B), see (Everitt et al. 2011). Following Schiff, a gyroscope in orbit around the Earth — an almost circular polar orbit in the case of the GP-B satellite at an altitude of about 640 km — is subject to two main relativistic precessions: a drift in the orbital plane, i.e., the de Sitter or geodetic precession, and a frame-dragging effect perpendicular to the orbital plane, see (Schiff 1960). This frame-dragging, also known as Schiff dragging, is due to the Earth's rotation and it is therefore related with the orbit dragging, i.e., with the Lense-Thirring effect. GP-B was equipped with four cryogenic gyroscopes. These were almost perfect homogeneous spheres with a tolerances better than 1 part per million. Each gyroscope was coated with a very thin layer of superconducting niobium. The gyroscopes were included inside a dewar of 2440 liters of superfluid helium at a temperature of 1.8 K. GP-B has provided a measurement of the frame-dragging effect and of the geodetic effect in agreement with the GR predictions with accuracies of about 19% and 0.28%, respectively.

3.2. Measurement of the GR advance of the argument of pericenter and of the PPN parameters β and γ

The GR precession of the argument of pericenter of a satellite tracked via SLR has been the subject of many investigations since the 70s of the last century. It was D.P. Rubincam that, in 1977, first attacked the problem of the precession of LAGEOS pericenter provoked by the Earth's gravitoelectric field, see (Rubincam 1977).

Rubincam concluded that, at that time, the relativistic shift was too small to be separated from other perturbations, such as the direct radiation pressure and the atmospheric drag; however he also underlined that an improved knowledge of the perturbations "*may permit the relativistic perigee shift to be measured in the near future, although the small orbital eccentricity may make determination of the argument of perigee difficult*".

Indeed, in the case of the pericenter ω, the observable is $e\dot{\omega}$; therefore, the larger the eccentricity e, the better the determination of the argument of pericenter ω. In 1977, the role of the several non-gravitational perturbations at work on the LAGEOS satellite was not yet well established, and Rubincam had, among the many researchers involved on this topic, a key role in their understanding during the subsequent years. For instance, thermal effects have been later discovered to play a fundamental role in explaining a large fraction of the observed decay of the semi-major axis of the two LAGEOS satellites (see e.g. (Rubincam 1987, Rubincam 1988, Scharroo et al. 1991)), while a smaller role is played by the neutral and charged particle drag. In particular, the Yarkovsky–Schach effect is responsible for several long-period perturbations on the satellite argument of pericenter, with an amplitude inversely proportional to the eccentricity e of the satellite; see Section 6.2 below.

A step forward in estimating the relativistic contribution to the advance of the pericenter of LAGEOS was done in 1992 by (Ciufolini & Matzner 1992). These authors, based on a measurement of LAGEOS pericenter advance at a 10% level over a time span of about 13 years (from a private communication by R. Eanes (CSR/Texas), see their Ref. [51]), performed an analysis of the main systematic errors due to the even zonal harmonics of the Earth's gravitational field. They considered the GEM-L2 and GEM-T1 models — see (Lerch, Klosko, Patel & Wagner 1985, Lerch, Klosko, Wagner & Patel 1985, Marsh et al. 1988) — and found an upper bound value of about 20% for the error of the shift of the pericenter with respect to the relativistic precession. In particular, they considered the covariance matrix of the two fields applied to their formal errors in order to account for the correlations among the coefficients. Therefore, their result can be expressed as:

$$\epsilon_\omega - 1 \approx (0 \pm 0.1) \pm 0.2, \tag{31}$$

where ϵ_ω represents the GR normalized precession due to the Earth's gravitoelectric field, with $\epsilon_\omega = 1$ in Einstein's GR and $\epsilon_\omega = 0$ in Newtonian classical physics.

It is important to stress that this 20% estimate for the error budget due to the systematic effects has to be considered for this analysis, at that epoch, as a lower

limit. Indeed, (Ciufolini & Matzner 1992) have not explicitly considered neither other gravitational error sources on the argument of pericenter — such as the time dependency of the even zonal harmonics, or the contribution from the odd zonal harmonics as well as that from the tidal effects — nor the non-gravitational perturbations. The authors have simply considered in their 20% estimate also a few percent contribution from other minor perturbations, as described in (Cohen et al. 1985), but not updated for that time.

In the subsequent years, and very strangely, no explicit measurement of the GR pericenter advance of an Earth satellite has never been performed, and only new estimates of the error budget for such a measurement were published, see e.g. (Iorio et al. 2002, Lucchesi 2003*a*, Lucchesi 2011) (this last work was presented at COSPAR2006, see (Lucchesi & Peron 2006)). The value of these works lies in focusing attention to a better consideration of the role played by the main systematic effects produced by the perturbations due to the gravitational and non-gravitational forces in the error budget of a measurement of the GR precession of the pericenter.

It was only in 2010 that a work focusing on the explicit measurement of the GR advance of LAGEOS II argument of pericenter was performed, see (Lucchesi & Peron 2010). The result was:

$$\epsilon_\omega - 1 \simeq (0.28 \pm 2.14) \times 10^{-3} \pm 2 \times 10^{-2}. \tag{32}$$

This result was based on a 13-year analysis of the orbit of the LAGEOS II satellite with the inclusion of the EIGEN-GRACE02S model for the Earth's gravitational field in the POD of the satellite. The LAGEOS II satellite was used because of its larger eccentricity ($e_{\rm II} \simeq 0.014$) with respect to that of LAGEOS ($e_{\rm I} \simeq 0.004$). As in the case of the previously described measurements of the Lense-Thirring effect, the GEODYN II software was used for the satellite data reduction.

As we can see from Eq. (32), the authors obtained, from their best fit of the integrated residuals of the satellite pericenter, a discrepancy of about 0.03% with respect to the prediction of GR, with an error of about 0.2% from the result of a sensitivity analysis. Finally, based on the previous estimate of the systematic effects provided in (Lucchesi 2003*a*) and in (Lucchesi 2011), (Lucchesi & Peron 2010) have preliminarily fixed the error budget of the measurement at the level of 2%, mainly dominated by the uncertainty in the quadrupole coefficient J_2.

In a subsequent re-analysis of the LAGEOS II orbit over the same time span of about 13 years, (Lucchesi & Peron 2014) have provided a new — and more precise — measurement of the GR advance of the satellite argument of pericenter, together with a very accurate analysis of the main systematic effects. The new result was:

$$\epsilon_\omega - 1 \simeq (-0.12 \pm 2.14) \times 10^{-3} \pm 2.54 \times 10^{-2}. \tag{33}$$

As we can see from Eq. (33), the discrepancy with respect to the slope of the integrated residuals of the pericenter predicted by GR has been reduced to 0.01%, a factor of three smaller than the result of the previous measurement. The very accurate estimate of the

error budget gives a value of 2.54%, slightly larger than the 2% previously fixed. This error budget is dominated by the uncertainty due to the first even zonal harmonic J_2, with an impact on the pericenter precession of about 2.27% of the prediction of general relativity. We refer to (Lucchesi & Peron 2014) for a deeper insight into the details of the error budget.

It is important to stress that in the framework of the PPN parameters the parameter ϵ_ω may be interpretated as a combination of the two post-Newtonian parameters β and γ (see Section 2), that is:

$$\epsilon_\omega \simeq \frac{|2+2\gamma-\beta|}{3}. \tag{34}$$

Therefore, the quoted measurements, in particular those of Eqs. (32) and (33), should be considered as a direct measurement of such a combination of the PPN parameters in the field of the Earth.

In particular, we can compare the result shown in Eq. (33) with analogous measurements from experiments performed in the solar system with the tracking of planets and of probes around planets or during flybys. A first and very long series of measurements in the case of the perihelion advance of Mercury was performed by Shapiro and collaborators, see (Shapiro et al. 1972, Shapiro 1990). They obtained:

$$\frac{|2+2\gamma-\beta|}{3} - 1 \simeq (\pm 1.0 \cdot 10^{-3}) \pm 2 \cdot 10^{-2}. \tag{35}$$

This previous and very important test of GR was performed with the radar ranging technique and based on the measurement of the echo delay between the Earth and Mercury in the period between 1966 and 1990.

Other constraints for the perihelion advance have been indirectly obtained from the ephemerides of the solar-system bodies. These ephemeris are computed numerically on the basis of relativistic equations of motion and are improved, for what concerns masses and distances of the considered bodies, with the tracking data of interplanetary probes, see for instance (Pitjeva 2009, Fienga et al. 2009). From this global fit of solar system bodies constraints on the advance of the perihelion of the planets produced by GR are given. From the cited papers (see also references therein) we can infer the following precision for the β and γ combination:

$$\frac{|2+2\gamma-\beta|}{3} - 1 \simeq \pm 2 \cdot 10^{-4}. \tag{36}$$

The real accuracy of such result is probably reduced because of several systematic effects.

3.3. Constraints on alternative theories for the gravitational interaction

As highlighted in Section 1, tests for non-Newtonian gravity and for a possible violation of the Weak Equivalence Principle are strongly related (see e.g. (Fischbach & et al. 1986, Adelberger et al. 2003)) and represent a powerful approach in order to validate GR with respect to other (proposed) alternative theories of gravity. In the following, we summarize the constraints obtained so far in this context from the SLR measurements of the orbit of the two LAGEOS satellites and their subsequent analyses.

3.3.1. Constraints on New Long Range Interactions Violations of the inverse–square law by very weak New Long Range Interactions (NLRI) are usually described by means of a Yukawa–like potential with strength α and range λ and transmitted by a field of very small mass $\mu = \hbar/\lambda c$:

$$V_{\rm Yuk} = -\alpha \frac{G_\infty M_\oplus}{r} e^{-r/\lambda}, \quad \alpha = \frac{1}{G_\infty}\left(\frac{K_\oplus}{M_\oplus}\frac{K_s}{m_s}\right). \tag{37}$$

Here G_∞ represents the Newtonian gravitational constant, $M_\oplus$ and m_s are the mass of the primary body (the Earth) and of the satellite, r is their separation, c the speed of light and $\hbar$ the reduced Planck constant. The strength α depends both on the mass-energy content of the sources and on their coupling strengths, $K_\oplus$ and K_s respectively. Indeed, depending on the nature of the coupling strengths that enter in Eq. (37), we can simply have a metric gravitational theory or a more complex non-metric theory. The former case happens when $K_\oplus$ and K_s are proportional to the mass-energy content of the two sources, i.e., to $M_\oplus$ and m_s respectively. Conversely, in the latter case, the coupling strengths are proportional to some exotic (conserved) charge or to other forms of energy. In these cases, in addition to violations of the inverse-square law also EEP violations will be present. Threfore, NLRI may have various origins, from modifications of the gravitational interaction with respect to Einstein's GR to modern theories for particle physics and string theory. For instance, NLRI may be thought of as the residual of a cosmological primordial scalar field related with the inflationary stage (Damour et al. 2002*a*). This is the so-called dilaton scenario, in which the dilaton is a scalar partner of the spin-2 graviton, see also (Damour et al. 2002*b*).

Among the different techniques useful for the search of this additional physics at the various scales, the accurate measurement of the pericenter shift of binary systems, such as the Earth and an orbiting satellite, may be used to test for a NLRI with a characteristic range comparable with the system semimajor axis, see (Nordtvedt 1998, Nordtvedt 2000). In particular, the impact on LAGEOS II argument of pericenter of the main systematic error sources in this context was evaluated in (Lucchesi 2003*a*, Lucchesi 2011), see also (Iorio et al. 2002). Subsequently, (Lucchesi & Peron 2010, Lucchesi & Peron 2014) have constrained a possible NLRI at a range λ close to 1 Earth radius from their measurement and error budget of the pericenter advance of LAGEOS II. Indeed, (Lucchesi & Peron 2014) found a maximum secular effect on the pericenter given by:

$$< \dot\omega^{\rm Yuk} >_{2\pi} \simeq 8.29 \cdot 10^{11}\alpha \quad [\rm mas/yr] \tag{38}$$

which corresponds to the peak value at a range $\lambda = 6,082$ km. Consequently, from their result of Eq. (33) they found an upper bound for the strength α of a possible long-range interaction given by:

$$|\alpha| \simeq |(0.5 \pm 8.0) \pm 101| \cdot 10^{-12} \tag{39}$$

where the last contribution is due to the systematic errors.

It is worth mentioning that previous results using Earth-LAGEOS and Lunar-LAGEOS measurements of GM were confined at the level of 10^{-5} and 10^{-8} respectively, see e.g. (Li & Zhao 2005). Therefore, this result represents a huge improvement in the constraint of the strength α at 1 Earth radius and it is very competitive with those obtained with Lunar Laser Ranging (LLR) measurements at a characteristic scale of about 60 Earth radii, where $\alpha \simeq 2 \cdot 10^{-11}$, see (Müller et al. 2008, Murphy 2013) and references therein.

3.3.2. Constraints on Non-Symmetric and Torsional theories When a modification of GR is proposed, the equation of motion of a test body is no longer the standard *geodesic equation* because of the presence of some new attribute. If, as a consequence, this new attribute is responsible for a secular effect on one of the orbital elements of a satellite, we are able to measure the long-term behaviour of such element and place constraints on the existence of the attribute responsible of its further — with respect to that of GR — time evolution. In the following, we show the constraints obtained with the two LAGEOS satellites in the case of theories of gravitation characterized by non–symmetric connection coefficients $\Gamma^{\gamma}_{\alpha\beta}$.

For instance (Moffat 1979), see also (Moffat & Woolgar 1988), suggested the possibility of a Non-Symmetric Gravitation Theory (NSGT). The motivation was to follow Einstein's idea to unify gravitation and electromagnetism introducing a non-symmetric fundamental tensor. As a consequence, for the pericenter rate of a binary system consisting of a primary $\mathcal{B}$ and a satellite $\mathcal{S}$, the authors obtained an additional contribution with respect to Schwarzschild precession given by:

$$\dot{\omega}^{\rm Mof} = \frac{3(GM)^{3/2}}{c^2 a^{5/2}(1-e^2)}\left[\mathcal{C}_{\mathcal{BS}}\frac{c^4\big(1+e^2/4\big)}{\big(GMa(1-e^2)\big)^2}\right], \tag{40}$$

with $\mathcal{C}_{\mathcal{BS}}$ depending on the NSGT charges of the two bodies: $\ell^2_{\mathcal{B}}$ and $\ell^2_{\mathcal{S}}$. In the case of the Earth-LAGEOS system a first constraint in $\mathcal{C}_{\mathcal{BS}} \rightarrow \mathcal{C}_{\oplus Lageos}$ was given by (Ciufolini & Matzner 1992) using the total uncertainty in the calculated precession of the satellite pericenter. The authors obtained:

$$\mathcal{C}_{\oplus\rm Lageos} \leq (0.16km)^4. \tag{41}$$

Subsequently, (Lucchesi 2003*a*) was able to improve such result on the basis of an accurate analysis of the main systematic effects on the LAGEOS II pericenter rate. The result was:

$$\mathcal{C}_{\oplus\rm Lageos\ II} \leq (0.087km)^4. \tag{42}$$

Finally, (Lucchesi & Peron 2014), by imposing that their estimated precision and accuracy in the LAGEOS II pericenter rate measurement of Eq. (33) is due to the discrepancy between the Moffat NSGT and Einstein's GR, obtained the following upper bounds:

$$\mathcal{C}_{\oplus\rm Lageos\ II} \leq (0.003km)^4 \pm (0.036km)^4 \pm (0.092km)^4. \tag{43}$$

The larger upper bound, that arises from the analysis of the systematic errors, is comparable with the result obtained in (Lucchesi 2003*a*). In conclusion, these results are all consistent with a null result, hence they place very strong limits on a possible NSGT.

A second example of non-symmetric connection coefficients $\Gamma^{\gamma}_{\alpha\beta}$ is that due to a non-vanishing torsional tensor, as when a generalization of Einstein's GR may be obtained from a Riemann-Cartan spacetime (Hehl et al. 1976, Hammond 2002). Following (Mao et al. 2007) the presence of torsional effects in the Solar System should be tested experimentally. These authors developed a theory that parameterizes both metric and connection by a set of parameters that are able to describe torsional effects. Subsequently, the corrections to the pericenter longitude ($\varpi = \omega + \Omega$) produced by these possible spacetime torsions were computed in the WFSM limit in the case of a satellite orbiting the Earth and in the field of the Sun by (March et al. 2011*a*, March et al. 2011*b*). Considering only their corrections to Schwarzschild precession, the authors obtained:

$$\dot{\omega}^{\rm torsion} = \frac{3(GM)^{3/2}}{c^2 a^{5/2}(1-e^2)}\left(\frac{2t_2+t_3}{3}\right), \tag{44}$$

where t_2 and t_3 are two of the parameters (among the several) that describe the torsion effects. Then (Lucchesi & Peron 2014), with the results of their analysis, have been able to constrain these two parameters related with torsion. They obtained:

$$|2t_2+t_3| \simeq 3.5\cdot 10^{-4} \pm 6.2\cdot 10^{-3} \pm 7.49\cdot 10^{-2}, \tag{45}$$

to be compared with $|2t_2+t_3| \simeq 3\cdot 10^{-3}$ obtained by (March et al. 2011*b*) using the Mercury's perihelion shift measurement of (Shapiro 1990).

4. LARASE goals

In the previous two sections we have defined the theoretical limits of our field of investigation as well as the current state of the art of the best measurements of relativistic gravity in the field of the Earth by means of the SLR technique. In this section we will focus on the main objectives of LARASE.

The project denominated LARASE (LAser RAnged Satellites Experiment) aims to test the gravitational interaction in the WFSM limit of GR by means of very precise orbit determination for a set of laser-ranged satellites orbiting the Earth. In the family of the passive laser-ranged satellites, the two LAGEOS will still play a key role together with the recently launched LARES. The older LAGEOS (LAser GEOdynamic Satellite) was launched by NASA on May 4, 1976; LAGEOS II was jointly launched by NASA and ASI on October 22, 1992; finally LARES (LAser RElativity Satellite) was launched by ASI on February 13, 2012.

These satellites are spherical in shape, fully passive, and with a low area-to-mass ratio in order to minimize the non-gravitational accelerations acting on them. The two LAGEOS are almost twin satellites, with an area-to-mass ratio of about $6.95\cdot 10^{-4}$

m^2/kg and a radius of about 30 cm. LARES has an area-to-mass ratio smaller by a factor of 2.6 with respect to that of the two LAGEOS, and a radius of about 18 cm. Indeed, it is made of a tungsten alloy, and it represents the densest object ever launched in space, see Figure 2.

Figure 2. Picture of the LARES satellite (credits from LARES Mission: CC BY 3.0; see also www.lares-mission.com/gallery.html). LARES is made of a unique piece of tungsten (THA-18N, composition 95% of W and 5% of Cu and Ni) and its surface is covered with 92 CCRs for SLR tracking. The CCRs mounting system is quite similar to that of the two LAGEOS, the most important difference is that the mounting rings and the screws are made of the same tungsten alloy of the satellite. The satellite radius is 18.2 cm and its mass is about 386.8 kg. The satellite orbit is almost circular with a semi-major axis of about 7820 km (corresponding to an orbital period of about 6883 s). LARES has been lunched with the qualification flight of the new European launcher VEGA.

In Table 2 the mean elements for the three satellites are given for their semi-major axis a, eccentricity e and inclination i. The table also gives the satellites right ascension of the ascending node Ω and argument of pericenter ω, for a fixed reference epoch.

LARES was launched with the goal to provide — by combining in a suitable manner its POD with that of the two LAGEOS — a new and refined measurement of the Lense-Thirring effect at about 1% level, i.e., a factor of 10 better than the current constraints

Table 2. Mean Keplerian orbital elements of LAGEOS, LAGEOS II and LARES. The reference epochs at which right ascension of ascending node and argument of pericenter are estimated are MJD 48919 (October 24, 1992) for LAGEOS and LAGEOS II and MJD 55975 (February 18, 2012) for LARES, respectively.

Element	LAGEOS	LAGEOS II	LARES
Semi-major axis [m]	$1.227\,000\,320 \times 10^7$	$1.216\,207\,038 \times 10^7$	$7.820\,305\,76 \times 10^6$
Eccentricity	$4.433\,30 \times 10^{-3}$	$1.379\,805 \times 10^{-2}$	$1.195\,78 \times 10^{-3}$
Inclination [deg.]	109.84	52.66	69.49
Right ascension of the ascending node [deg.]	289.74	113.75	230.84
Argument of pericenter [deg.]	53.12	212.57	296.99

obtained with the two LAGEOS satellites only; we refer to (Ciufolini et al. 2009) and (Paolozzi & Ciufolini 2013) for details.

As we highlighted in Section 3, there are two fundamental ingredients needed for the POD of a satellite: i) the quality of the tracking observations of the orbit and ii) the quality of the dynamical models included in the software code for the orbit determination. Therefore, LARASE aims to improve the dynamical models of the currently best laser-ranged satellites, with special attention to the subtle and complex modelling of non-gravitational forces. These are non-conservative forces that depend (strongly) on the satellite structure — both external and internal — and on the way it interacts with the environment around it and the radiations hitting its surface.

The dynamical models for the non-gravitational perturbations are only partly included in the current best codes developed for the POD of passive laser–ranged satellites, such as the two LAGEOS. This means that an effort is needed to develop more accurate models, as well as new dedicated models for the LARES satellite, and then include them in the current codes for a more precise and accurate data reduction.

Among the various non-gravitational perturbations that need special attention, especially if we are interested in the joint analyses of the orbit of LARES with those of the two LAGEOS, we have to consider the thermal thrust forces and the drag perturbations due to both neutral and charged species at the altitude of interest.

The thermal thrust forces depend strongly on the satellite spin–axis orientation and rate, hence an accurate model for the spin evolution of each satellite is needed. Moreover, in order to account correctly for the various thermal forces acting on the surface of a satellite, a detailed structural and thermal model is also needed. These forces have to be considered carefully both for the two LAGEOS and the new LARES. Conversely, the drag forces are especially important for LARES because of its (much) lower height with respect to the two LAGEOS, about 1450 km vs. 5900 km.

Beside the non-gravitational perturbations, also the gravitational perturbations need to be carefully considered in order to reduce the impact of their systematic

Table 3. Magnitude of the main disturbing accelerations $[m/s^2]$ on LAGEOS II and on LARES. Derived from (Milani et al. 1987).

Effect	Estimate	LAGEOS II	LARES
Earth's monopole	$\frac{GM_\oplus}{r^2}$	2.69	6.51
Earth's oblateness	$3\frac{GM_\oplus}{r^2}\left(\frac{R_\oplus}{r}\right)^2 \bar{C}_{2,0}$	-1.1×10^{-3}	-6.4×10^{-3}
Low-order geopotential harmonics	$3\frac{GM_\oplus}{r^2}\left(\frac{R_\oplus}{r}\right)^2 \bar{C}_{2,2}$	5.4×10^{-6}	3.2×10^{-5}
High-order geopotential harmonics	$19\frac{GM_\oplus}{r^2}\left(\frac{R_\oplus}{r}\right)^{18} \bar{C}_{18,18}$	1.4×10^{-12}	4.6×10^{-9}
Moon perturbation	$2\frac{GM_\bullet}{r_\bullet^3} r$	2.2×10^{-6}	1.4×10^{-6}
Sun perturbation	$2\frac{GM_\odot}{r_\odot^3} r$	9.6×10^{-7}	6.2×10^{-7}
General relativistic correction	$\frac{GM_\oplus}{r^2}\frac{GM_\oplus}{c^2}\frac{1}{r}$	9.8×10^{-10}	3.7×10^{-9}
Atmospheric drag	$\frac{1}{2}C_D\frac{A}{M}\rho V^2$	-2.6×10^{-13}	-1.3×10^{-11}
Solar radiation pressure	$C_R\frac{A}{M}\frac{\Phi_\odot}{c}$	3.2×10^{-9}	1.2×10^{-9}
Albedo radiation pressure	$C_R\frac{A}{M}\frac{\Phi_\odot}{c}A_\oplus\left(\frac{R_\oplus}{r}\right)^2$	3.5×10^{-10}	2.4×10^{-10}
Thermal emission	$\frac{4}{9}\frac{A}{M}\frac{\Phi_\odot}{c}\alpha\frac{\Delta T}{T_0}$	2.8×10^{-11}	not available
Dynamic solid tide	$3k_2\frac{GM_\bullet}{r_\bullet}\left(\frac{R_\oplus}{r_\bullet}\right)^2\frac{R_\oplus^3}{r^4}$	3.7×10^{-6}	2.2×10^{-5}
Dynamic ocean tide	~ 0.1 of the dynamic solid tide	3.7×10^{-7}	2.2×10^{-6}

uncertainties on the relativistic measurements in which we are interested. In particular, with regard to the LARES, because of its relative low altitude — compared to that of the two LAGEOS — we need to account in the modelling of the Earth's gravitational field for a much higher number of spherical harmonic terms, up to degree ℓ and order m of about 90, compared to ℓ and m of about 30 for the two LAGEOS. Moreover, also the Earth's tides (both solid and ocean) will impact more deeply the satellite orbit. We refer to Table 3 for an order-of-magnitude comparison of the main gravitational and non-gravitational perturbations acting on LAGEOS II and on LARES.

As we can see, because of its smaller semi-major axis (about 7820 km vs. 12162 km), the perturbing effects on LARES are usually larger than those on LAGEOS II. Indeed, in the case of the non-conservative forces, the smaller area-to-mass ratio plays a significant role only in the case of the direct solar radiation pressure. In the case of the drag acceleration, the benefit is cancelled by the much larger atmospheric density ρ and the higher speed V of LARES, see Section 6.3, while in the case of the albedo perturbation the benefit is nulled by the $1/r^2$ dependence on the Earth's distance.

However, it is precisely thanks to the lower area/mass ratio of LARES that the

Table 4. Rate (mas/yr) of the different types of secular relativistic precession for the two LAGEOS satellites and LARES (1 mas/yr = 1 milli–arc–second per year). These rates have been computed using the mean values of the orbital elements shown in previous Table 2.

Rate [mas/yr]	LAGEOS	LAGEOS II	LARES
$\dot{\omega}^{\rm Schw}$	3278.78	3352.58	10 110.13
$\dot{\omega}^{\rm LT}$	31.23	−57.33	−124.53
$\dot{\Omega}^{\rm LT}$	30.67	31.51	118.47
$\dot{\Omega}^{\rm dS}$	17.60	17.60	17.60

disturbing effects due to the non-gravitational perturbations, independently of the lower height of the satellite, are comparable with those of the two LAGEOS. This allows one to infer an orbit determination of LARES not too much different from that obtainable for the two LAGEOS. See Section 5.2.

With regard to the relativistic measurements to be performed in the near future, a way to test the predictions of Einstein's geometrodynamics with respect to those due to other metric theories is through the measurements of the so-called PPN parameters (Section 2). In particular, among these parameters, major goals of our investigation are γ, β, α_1 and α_2. Because of the importance of the Lense-Thirring precession, also the parameter μ will be subject of our new investigations. Indeed, in Section 2 we have only focused on the distinction between intrinsic gravitomagnetism and the gravitomagnetic-like effect that arises from a motion on a static background, i.e., the geodetic precession. However, very interesting are the astrophysical and cosmological implications associated with the frame-dragging effect, see e.g. (Ciufolini & Wheeler 1995), that enhance the importance of a very precise measurement of this relativistic precession, also in the WFSM limit.

Through a POD, these relativistic parameters may be determined in two distinct ways: i) directly, as solved-for parameters or, ii) indirectly, by the measurement of the relativistic precessions that impact the three Euler angles that define the orientation of the orbit in the inertial space (see Sections 2 and 3).

In Table 4, the values of the secular relativistic effects on the pericenter and nodal rate of such satellites in the case of their nominal keplerian elements a, e and i (see Table 2) are shown.

In the case of the argument of pericenter, the dominant effect is the gravitoelectric precession, analogous to Mercury perihelion precession in the field of the Sun, with a smaller contribution from the gravitomagnetic effect. As we can see, due to the fact that the gravitomagnetic precession is inversely proportional to the cube of the distance, in the case of LARES the relativistic Lense-Thirring precessions of the argument of pericenter and of the right ascension of the ascending node are larger than those of the two LAGEOS satellites by a factor close to four.

Concerning the effects on the satellite orbital motion produced by a (possible)

preferred frame, in particular from the α_1 parameter, these have been investigated by (Damour & Esposito-Farèse 1994). The main effects consist of a very complex secular evolution of the orbit eccentricity vector $\mathbf{e}$ — the so-called Runge-Lenz (or Laplace) vector (which is a constant of motion in the ideal two-body and Newtonian problem) — and on a yearly oscillation in the longitude of the satellite. These authors have shown that satellites characterized by particular values of their orbit inclination i with respect to the Earth's equator have the potential to improve the current limits on α_1 ($\simeq 1 \cdot 10^{-4}$) by about two orders of magnitude. Luckily for this goal, the orbital inclinations of the two LAGEOS satellites, as well as that of LARES, are very close to these critical inclinations. A similar work has been performed by (Vokrouhlický & Métris 1998), that have also considered the measurement of the α_2 parameter. See also (Nordtvedt 1999).

Moreover, concerning the constraints to alternative theories for the gravitational interaction, it will be very interesting to compare the results of gravitational physics tests from the SLR technique measurements with those of the LLR ones. In addition to the previously cited PPN parameters and to the strength α of a possible Yukawa-like interaction, this comparison will be relevant about the constraints on possible violations of the WEP and of the strong equivalence principle (SEP), as well as on the possible time variation of the gravitational constant G. The goal is not simply to see whether one technique provides better and more robust measurements — of course in this sense LLR is much better for EEP tests — but to test the characteristic methods of one technique (the LLR one) as compared to the other one and to verify the impact of different systematic error sources in the results. Indeed, while the techniques are very similar, some of the physical models involved and the orbits are different. This means that the main perturbations have a different role in the two cases. For instance, in the case of SLR the non-gravitational perturbations play a major role, while they are negligible for the Moon. Conversely, while some gravitational perturbation is of primary importance in the case of LLR, it is negligible for SLR (as for the tidal evolution effects).

Of course, and similarily, both the Earth-Moon and the Earth-LAGEOS systems are in free fall in the field of the Sun; but the orbit of a LAGEOS-like satellite is more strongly tied to the Earth than the orbit of the Moon, and this has a deep consequence in the measurement of several tiny relativistic effects. In case of common models for some parameters, such as for the positions of the stations that perform both LLR and SLR tracking, the more precise measurements of such parameters from one technique could help in improving the results obtainable with the other. For further details about this possible comparison between the two techniques we refer to (Nordtvedt 2001) and to (Nobili et al. 2008).

One crucial aspect that LARASE should clearly address is represented by a reliable estimate of the systematic uncertainties that contribute to the error budget of the various relativistic measurements that will be performed in the future. As previously outlined, these systematic uncertainties are, in their nature, both of gravitational and non-gravitational origin. In particular, it will be of great importance to clearly identify possible correlations among estimates of the relativistic precessions and those of other

physical quantities that are able to mimic, because of their secular (or very long periodic) behavior, a secular trend like those of the relativistic effects.

In conclusion, once the above improvements in the dynamical models will be reached, it will be possible to test more precisely and accurately Einstein's theory of gravitation with respect to the other metric (and also non-metric) theories that have been proposed for the interpretation of the gravitational interaction, and to go beyond the present best measurements (and kinds of tests) performed so far.

5. Precise orbit determination and dynamical models

The precise determination of the orbit followed by a satellite is a very common task and basic to every space mission (for the relevant methods, see e.g. (Montenbruck & Gill 2000, Tapley et al. 2004, Milani & Gronchi 2009)). Essentially, it amounts to using some observable (it could be, e.g., instantaneous position or velocity) in order to obtain position and velocity of the object as a function of time (the so-called *ephemerides*) in a given time span. The tracking data (our observables) contain the information associated with the orbit itself, as well as to the satellite dynamics, the measurement procedure and the observational "constraints" (i.e., stations position, reference frames). This information has to be extracted in some way from the data. The problem is not trivial, considering the relative magnitudes of the effects involved (see Table 3) and the fact that aliasing among parameter estimates has to be avoided as much as possible.

A direct comparison between the data precision (at the mm level), the orbit reconstruction accuracy (at the cm level) and the expected magnitude of the effects being sought for (see Section 3 and Table 4) shows that the measurements are feasible, given a proper modellization of the satellite dynamics. At the end, the orbit determination reduces to a proper estimation scheme, such as least squares, following the general equations (22) introduced in Section 3 (see e.g. (Kaula 1966)).

A least-squares solution of Eq. (22) amounts to minimizing the *residuals* $O_i - C_i$, at the same time solving for the corrections $\mathrm{d}P_j$ (*differential correction procedure*). This procedure leads, for each considered time period (*arc*), to estimates of both the state vector (initial conditions: position $\mathbf{x}$ and velocity $\dot{\mathbf{x}}$) and a selected set of model parameters. Among several software packages developed for this purpose, we use the NASA/GSFC GEODYN II (Pavlis & et al. 1998, Putney et al. 1990). This software is dedicated to satellite orbit determination and prediction, geodetic parameters estimation, tracking instruments calibration, and many other applications in the field of space geodesy.

In LARASE, the analysis strategy is based on a multi-arc POD, in which the overall time span of the analysis is divided into a number of successive (short) arcs, not causally connected, and then, for each of them, the satellite state vector is estimated along with a set of relevant model parameters. The arc length (dependent on the satellite being analyzed) is chosen as a compromise between having a sufficient number of data points and small not modelled effects not accumulating too much over this period, and, at the

same time, long enough that the accumulated unmodelled secular relativistic effects are larger than the corresponding error in the measurements and models.

A basic choice of our analysis is the use of the residuals in order to recover the relativistic effects (or whatever physical quantity deemed useful for the purposes of the analysis). The residuals provide a measure of the discrepancy between experimental data (i.e., the SLR observations) and models; by purposely not including a selected physical phenomenon into the modelling set, the residuals time series is expected to contain signatures of the effect itself. Since the basic observable is distance, the residuals are, naturally, on station-satellite distances. Being interested in the effects of GR on the orbital elements of a satellite, we employ the method outlined in (Lucchesi & Balmino 2006) in order to obtain, for each element, the time series of its corresponding residuals. This is the method that has been used in the past in various tests of relativistic dynamics (Ciufolini et al. 1996, Ciufolini, Lucchesi, Vespe & Chieppa 1997, Ciufolini et al. 1998, Ciufolini & Pavlis 2004, Ciufolini et al. 2006) and, more recently, in (Lucchesi & Peron 2010, Lucchesi & Peron 2014).

As well known in space geodesy studies, a non-negligible number of model parameters are usually estimated in analyses which involve both geodetic and geophysical applications. Conversely, in the case of measurements in the field of fundamental physics, only a small number of model parameters are estimated, namely those most directly related to the particular orbit of the chosen satellite. Consequently, the other (environment related) parameters, are selected as *consider parameters*, i.e., the ones which are already known with sufficient accuracy from other sources. This approach is in line with our strategy of recovering the sought-for signals from the orbital residuals and, at the same time, it considerably simplifies the mathematical structure of the problem being solved. In particular, we do not include (apart from some particular case) the so-called *empirical accelerations* in the set of models used to fit the SLR observations. Experience shows that these can bias the estimate procedure and corrupt the residuals time series.

5.1. Dynamical models

Even though the geodetic satellites here considered are very simple ones, their orbits nonetheless point — at the level of SLR NP precision — to a rather complex dynamics. As described in Section 4, the effects at play can be broadly divided into gravitational and non-gravitational ones. The main ones are listed in Table 3, along with their magnitudes in the case of LAGEOS II and LARES; for extended discussions on them see (Milani et al. 1987, Montenbruck & Gill 2000). Models for them must be included in the satellite equation of motion for a precise determination of its trajectory, along with a consistent description of the measurement procedure (observation equation) and of the reference frames involved.

We are trying to follow as much as possible established modelling conventions and resolutions, namely those from the International Earth Rotation and Reference Systems

Table 5. Modelling setup as included in the analysis. Three groups are indicated: gravitational effects, non-gravitational ones and reference frames.

Model for	Model type	Reference
Geopotential (static)	EGM96, EIGEN-GRACE02S	(Lemoine & et al. 1998, Reigber et al. 2005
Geopotential (time-varying, tides)	Ray GOT99.2	(Ray 1999)
Geopotential (time-varying, non tidal)	IERS Conventions (2010)	(Petit & Luzum 2010)
Third-body	JPL DE-403	(Standish et al. 1995)
Relativistic corrections	Parameterized post-Newtonian*	(Huang et al. 1990)
Direct solar radiation pressure	Cannonball	(Pavlis & et al. 1998)
Earth albedo	Knocke-Rubincam	(Rubincam et al. 1987)
Earth-Yarkovsky	Rubincam (1987-1990)	(Rubincam 1987, Rubincam 1988, Rubinca
Neutral drag	NRLMSISE-2000	(Picone et al. 2002)
Spin	LARASE (2014)	To be published
Stations position	ITRF2008	(Altamimi et al. 2011)
Ocean loading	Schernek and GOT99.2 tides	(Pavlis & et al. 1998, Ray 1999)
Earth Rotation Parameters	IERS EOP C04	(International Earth Rotation Service n.d.)

*In fact, as explained in the text, these corrections have not been included in the modelization setup u

Service (IERS) and the International Astronomical Union (IAU). The IERS Conventions (2010) (Petit & Luzum 2010) constitute the general framework for reference systems related issues and measurement models. The IAU 2000 Resolutions (Soffel et al. 2003) recommend the use of a well-defined relativistic framework in dealing with celestial mechanics in the Solar System. We stress that such conventions and resolutions are usually updated to cope with the state of the art in observation and theory. So, in a sense, dealing with them is a continuous task: indeed, a non-negligible part of the activities described in this article is related to having a modellization set as much as possible in line with current research in the field.

In Table 5, the models currently implemented in GEODYN that we are going to use in our data reductions are shown. These models include the GR corrections in the PPN formalism discussed in Section 2. Of course, such corrections need to be removed from the setup in order to recover the secular precessions provoked by GR in the residuals time series. With regard to the perturbation provoked by the Yarkovsky-Schach effect (see Section 6.2), we will take into account such effect *a posteriori*, when necessary, with an *ad hoc* routine. Concerning the satellites spin vector evolution, we use our own model, see Section 6.1.

In general, we have at our disposal a number of independent routines to model

separately the main non-gravitational perturbations, namely for:

- direct solar radiation;
- Earth's albedo radiation;
- Yarkovsky–Schach thermal effect;
- Earth–Yarkovsky thermal effect;
- asymmetric reflectivity.

With regard to the neutral drag perturbation, besides the models included in GEODYN, in order to handle its disturbing effects we make use of the software SATRAP. This is a dedicated code that is able to load (and easily handle) several models for the Earth's atmosphere; see Section 6.3 for details.

5.2. Preliminary orbit determination

In the context of the LARASE activities, we extended the time span for the analysis of the orbit of the two LAGEOS satellites up to all 2014, starting from the October 24, 1992, two days after LAGEOS II launch. We started in parallel an analogous analysis activity related to LARES data. Whenever possible, the analysis setup has been the same for the three satellites. This is described with some detail in Section 5.1. We just notice the update of the terrestrial reference frame to its ITRF2008 version (Altamimi et al. 2011), including station eccentricities and discontinuities (due e.g. to earthquakes).

We also started an analysis with the goal to compare the gravity field models from the GRACE and GOCE missions (Beutler et al. 2003), in order to select the best solutions for the Earth's gravitational field to be used in our future analyses of the relativistic effects. The idea is to use the EIGEN-GRACE02S model, successfully used in previous measurements of the relativistic effects (see (Ciufolini & Pavlis 2004, Lucchesi & Peron 2014)), as a benchmark in order to compare the precision of the various models in the satellites orbit reconstruction (via their statistics comparison) and to infer their accuracy with an analysis of their systematic effects (role of the consider parameters).

Our preliminary analyses included a preparatory data reduction — over 14-day arcs for LAGEOS and LAGEOS II and 7-day arcs for LARES — of the range data for all three satellites, with a tailored modelling setup. Together with state vector and selected station biases, the radiation coefficient C_{R} and the corrections to polar motion $(X_{\mathrm{p}}, Y_{\mathrm{p}})$ and length of day (LOD) have been estimated; empirical acceleration components have been also used. The results of these analyses (expressed as post-fit RMS) are shown in Figure 3. LAGEOS and LAGEOS II orbits are recovered with a mean error roughly between 1 and 1.5 cm, while LARES orbit has a slightly higher error, roughly $\lesssim$2 cm; this is due to a currently non-optimal modelling for the dynamics of the newer satellite. The decreasing trend of the RMS of the range residuals obtained for the two LAGEOS, which approaches the 5 mm (mean) value at the end of the analyzed time span, is also in quite good agreement with the results obtained from the data reduction of the orbit of these satellites performed by the Analysis Centers of the ILRS network. We have

to notice that these rather good figures are being possible thanks to the inclusion of the empirical accelerations in the data reduction: corresponding analyses done without these terms (and also estimating a lesser number of parameters) show a rather higher error. This is not a surprise: it is an indication of the fact that some effect is still present in the residuals after the data reduction.

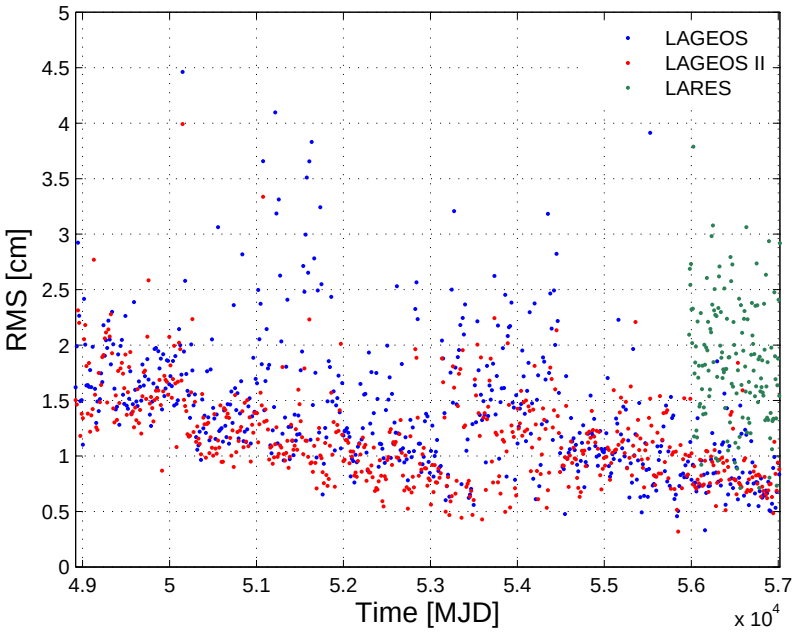

Figure 3. Data reduction outcome (expressed as post-fit RMS in cm) for LAGEOS, LAGEOS II and LARES tracking data. The time is given in Modified Julian Date (MJD). In the case of the two LAGEOS, the starting epoch (MJD 48919) corresponds to October 24, 1992, while, in the case of LARES, the starting epoch (MJD 55975) corresponds to February 18, 2012. The arc length is 14 days for LAGEOS and LAGEOS II, and 7 days for LARES. Notice the higher uncertainty associated with the LARES analysis, showing its currently non-optimal modelling.

The main purpose of the preliminary analysis has been obtaining a uniform and consistent orbit for each of the satellites, starting point for subsequent analyses.

6. Models improvement

In previous sections, we have described the state of the art of relativistic measurements with passive laser-ranged satellites, and we have highlighted the importance of having *good observations* as well as *good models* for the several perturbations (both gravitational and non-gravitational) on their orbit. Of course, the pair *good observations* and *good models* guarantees, at least in principle and *a posteriori*, a motion along a geodesic for the considered satellites.

In the following subsections we briefly focus on some of the aforementioned perturbations, highlighting their main characteristics and the difficulties to be overcome

in order to improve the current models. In so doing, we will outline some of the new results that we obtained from this work in the context of the LARASE activities. More details will be given in a number of forthcoming (and dedicated) papers.

6.1. Spin-axis

The rotational dynamics of passive satellites like the two LAGEOS has been deeply investigated in the past by many authors ((Bertotti & Iess 1991, Habib et al. 1994, Farinella et al. 1996, Vokrouhlický 1996, Williams 2002, Andrés et al. 2004, Andrés de la Fuente 2007)). Indeed, in order to improve the fit of the SLR range residuals, i.e. to obtain a precise solution for the orbit of a satellite, an accurate model of its spin vector behavior is needed because some non-gravitational perturbations depend on both the orientation and rate of the spin as previously highlithed, see also Section 6.2. This aspect reflects the coupling between the translational and rotational dynamics of the satellites.

The modelling of the spin vector evolution of the two LAGEOS satellites has proven to be a very complex problem, and it still is. Once the main external torques are identified, a correct mathematical formulation is needed that accounts for the characteristic periods of the several variables that enter in the spin evolution, namely i) the rotational period of the satellite, ii) its orbital period of revolution around the Earth, and iii) the sidereal period of Earth. However, these are not the only characteristic time scales to be considered. For instance, the thermal inertia τ of the satellite CCR plays a crucial role (see Section 6.2)‖. The main torques that influence the spin evolution of the two LAGEOS satellites are due to the Earth's gravitational and magnetic fields, respectively $\mathbf{\Gamma}_{\rm grav}$ and $\mathbf{\Gamma}_{\rm mag}$.

The effect of the first torque is like that of the lunisolar (Hipparcos) precession of the Earth's axis produced by the Moon and Sun gravitational pull on the equatorial bulge of the Earth's figure:

$$\mathbf{\Gamma}_{\rm grav} = -\frac{3}{4}\frac{n^2}{L^2}(I_z - I_x)(3\cos^2\theta - 1)(\hat{n}\cdot\mathbf{L})(\hat{n}\times\mathbf{L}), \tag{46}$$

where n represents the satellite mean motion, $\hat{n}$ the unit vector along the orbit normal, $\mathbf{L}$ is the satellite angular momentum, the angle θ represents the tilt between the symmetry axis of the satellite and its angular velocity direction, finally, I_z and I_x are the principal moments of inertia of the satellite, with $I_z < I_x$. We note that Eq. (46) is averaged over the proper rotation and precession of the satellite as well as over one orbital revolution; see (Farinella et al. 1996) for further details.

This gravitational torque arises because of the oblateness of the satellite due to the non-spherical distribution of its mass, of the order of a few % in the case of the two LAGEOS. Therefore, the knowledge of the internal structure of the satellites, namely of their moments of inertia along the principal axes, is of crucial importance in order

‖ In the literature of the LAGEOS satellites, the thermal inertia is also indicated as thermal lag time or thermal relaxation time of the CCRs.

to correctly model this effect. This gravitational torque produces a precession of the satellite spin around the Earth's rotation axis.

The torque produced by the Earth's magnetic field **B** is the hardest to be correctly modelled. This torque arises because the satellites are conductors moving in a variable magnetic field. The field induces eddy currents (Foucault currents), thence a magnetic moment $\boldsymbol{\mu}_{\rm m}(\mathbf{B})$ that in turn interacts again with the external field producing the magnetic torque:

$$\boldsymbol{\Gamma}_{\rm mag} = \boldsymbol{\mu}_{\rm m}(\mathbf{B}) \times \mathbf{B}. \tag{47}$$

This torque is responsible of two main effects: i) a drift of the satellite spin axis towards the Earth's magnetic dipole axis (this axis forms an angle close to 11° with respect to the Earth (nominal) rotation axis and rotates around it with the period of one sidereal day); ii) a despin of the satellite rate, i.e. an increase of the rotational period around the spin axis. The problem of the spin modelling of the two LAGEOS satellites has been attacked both using the full set of Euler equations, as in (Habib et al. 1994, Williams 2002), and using averaged equations for the torques, as in (Bertotti & Iess 1991, Farinella et al. 1996, Andrés et al. 2004). Very surprisingly, the best results have been obtained via the averaged equations method. Indeed, in this case the various authors have obtained a generally good agreement between the predictions of their model and the available observations of the spin orientation and rate, especially in the case of LA GEOS II (see e.g. (Andrés de la Fuente 2007)), in the (so-called) *rapid-spin case approximation* valid when the rotation period $T_{\rm rot}$ of the satellite is much smaller than its orbital period $T_{\rm orb}$.

In these models, following and extending the successful results of (Bertotti & Iess 1991), the magnetic torque is modelled in the *Landau-Lifshitz rotating frame* where the magnetic moment — more specifically the polarizability per unit volume — has been determined for a uniform sphere of radius ρ in the low frequency limit ($\rho \ll \delta$, δ being the penetration depth of the eddy currents), see (Landau & Lifshitz 1960). In particular, the LageOS Spin Axis Model (LOSSAM), as described in (Andrés de la Fuente 2007), is presently considered the best model for the prediction of the two LAGEOS satellites spin axis evolution in the rapid-spin case.

However, these successful models are valid only in the rapid-spin case approximation and their generalization to slow-spin rate regimes has never been done up to now. Anyway, in Sections B and C of (Andrés de la Fuente 2007) a way to generalize the spin model from the rapid-spin case to the slow-spin case is given in terms of both the excitation field to be considered at different frequencies as well as the treatment of the resonance condition between the proper rotation period of the satellite and its orbital revolution period. Moreover, in the case of LAGEOS the fit to the available observations is good but not so good as in the case of LAGEOS II; in the case of both satellites the agreement with the observations is worse during the first 10 years for LAGEOS and the first 3 years for LAGEOS II, see e.g. (Kucharski et al. 2013). This generalization is important not only for the two LAGEOS satellites, which have entered a regime that foresees a spin-orbit resonance condition, but also for the LARES satellite which was placed into its orbit with a quite high rotational period, about 12 s (Kucharski

et al. 2012), to be compared with about 1 s in the case of LAGEOS II and about 0.6 s for the older LAGEOS.

In our recent work we have deeply reviewed the interaction responsible of the magnetic torque that acts on the two LAGEOS satellites and the way the resultant magnetic moment depends on the various time scales characterizing this (difficult to model) disturbing effect. In particular, we have removed many of the simplifications at the basis of previous models. Moreover, by working on the original drawings of the LAGEOS II satellite and because we discovered that these are exactly the same as those of LAGEOS, we concluded that the two satellites are practically identical, differing only for the manufacturing tolerances and the material alloys. Therefore, we have been able to re-compute the mass of the two satellites and their moments of inertia thanks to a complete model of the two satellites at the finite elements. This enables us to obtain a better modelling of the gravitational torque on the two satellites.

In figure 4 and figure 5 are shown our new results in the case of the older LAGEOS satellite and their comparison with all the available observations: in red are shown the observations used by (Andrés de la Fuente 2007) following (Sullivan 1980, Avizonis 1997), while in green are shown the observations as derived by (Kucharski et al. 2013) from an *a posteriori* spectral analysis of LAGEOS range observations. The results are plotted in the J2000 inertial reference frame starting from the date of launch of LAGEOS up to May 16, 1998.

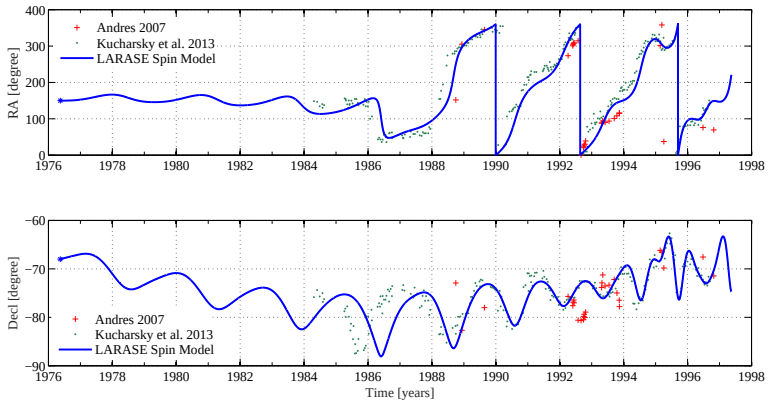

Figure 4. LAGEOS spin model (continuous line) and its comparison with observations: spherical coordinates (degrees) in the J2000 inertial reference frame. The upper plot represents the right ascension of the spin, while the lower plot is representative of its declination.

In figure 4 the spin orientation of LAGEOS (both right ascension and declination) is shown, while in figure 5 it is shown the behavior of the satellite rotation period. For a better comparison with the LOSSAM model, we have plotted our solution for the rapid-spin case. In addition to the main torques related with the Earth's gravitational and magnetic fields, we have also included in our model the torque related with the

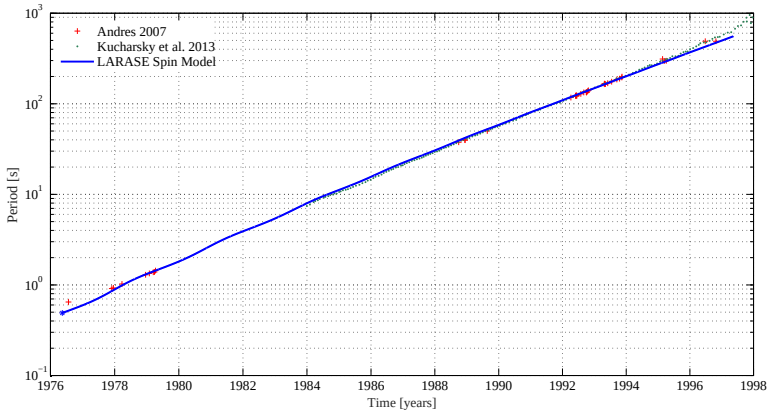

Figure 5. LAGEOS spin model and its comparison with observations: rotation period (seconds). The linear dependence on time in the semi–logarithmic scale is representative of the exponential de–spinning due to the magnetic torque.

asymmetric reflectivity between the two hemispheres of the satellite and that due to the offset between the satellite centre of mass and its geometrical center.

6.2. Thermal forces

Thermal forces are produced by an inhomogeneous temperature distribution over the satellite surface resulting in a thrust force due to the emitted radiation. Practically, these forces arise because of the finite thermal inertia of the satellite, especially of its CCRs. The two main sources of thermal forces are the Sun visible radiation, modulated by the satellite eclipses, and the Earth's infrared radiation. We presently focus on the first of the two cited forces, namely the Yarkovsky-Schach effect due to the Sun visible radiation.

Thermal forces depend on the satellite spin vector as previously described, giving different contributions on the satellite orbit as a function of both orientation and spin rate. When the fast spin assumption is valid for the satellite, a latitudinal-like distribution for the differential temperature across its surface can be assumed, and the consequent net recoil force will be directed along the spin–axis direction, in the "colder" pole direction (see e.g. (Afonso et al. 1989, Farinella et al. 1990, Scharroo et al. 1991, Slabinski 1996, Rubincam et al. 1997, Métris et al. 1997, Métris et al. 1999, Lucchesi 2002)). Conversely, if the assumption of a comparatively fast rotation of the spin is avoided, a longitudinal-like temperature distribution arises. Under this approximation, the thermal force will tilt from the spin-axis direction giving rise to additional "equatorial" components, and to more complicated equations to be solved, see (Farinella & Vokrouhlický 1996).

The transition from the fast-rotation approximation to the slow-rotation one is obviously dictated by the relationship among the three characteristic time scales described in Section 6.1: i) the rotation period, ii) the CCR thermal inertia, and iii) the

orbital period. In the case of the two LAGEOS satellites for the thermal inertia there are estimates in the range $2000 - 3000$ s (Afonso et al. 1989, Slabinski 1996, Lucchesi 2002) up to ≈ 9500 s (Andrés de la Fuente 2007), while their orbital period is about 13,300 s.

As soon as the rotation period of the satellite is less than the thermal inertia of the CCRs, the diurnal thermal asymmetry is negligible and the rapid-spin case approximation can be applied, as in (Afonso et al. 1989) or in (Slabinski 1996):

$$\mathbf{a}_z^{\mathrm{YS}} = -\frac{16}{9}\frac{A}{m}\frac{\epsilon_{\mathrm{ir}}\sigma}{c}T_0^3\Delta T\cos\theta_{\mathrm{s}}\Gamma(\lambda)\hat{s} \tag{48}$$

where $\hat{z}$ coincides with the satellite spin vector direction $\hat{s}$, ϵ_{ir} represents the CCR infrared emissivity, σ is the Stefan–Boltzmann constant, A and m are, respectively, the satellite cross-section and mass, T_0 is the average temperature of the satellite, ΔT is the temperature difference between the hotter and colder poles of the satellite, θ_{s} represents the angle between the spin vector direction and the Sun direction. Finally, $\Gamma(\lambda)$ represents the so-called physical shadow function of the satellite, with λ the satellite longitude over the orbital plane (argument of latitude) measured from the ascending node line. The purpose of this function is to model the decay of the sun radiation flux when the satellite enters the Earths shadow as well as the increase of this flux and, consequently, of the perturbative acceleration, when the satellite exits from the shadow. We refer to (Afonso et al. 1989, Métris et al. 1997) for further details.

Conversely, when the fast rotation approximation is not valid, the model developed by (Farinella & Vokrouhlický 1996) must be used because of its validity for any ratio of the three basic timescales previously cited. Therefore, we have a *seasonal-like* Yarkovsky-Schach effect when the fast spin approximation is valid, and a *diurnal-like* Yarkovsky-Schach effect when the former approximation is not valid.

With our new work on the thermal thrust forces we reviewed the impact of the Yarkovsky-Schach effect on the orbit of the two LAGEOS satellites — removing the fast spin approximation — following and extending the results of (Farinella & Vokrouhlický 1996). We have also started to review the entire thermal model of these satellites beginning from the work and the results of (Slabinski 1996) and (Andrés de la Fuente 2007). In particular, in the case of the Yarkovsky-Schach effect perturbation the following improvements have been obtained with respect to (Farinella & Vokrouhlický 1996):

(i) we completed their analysis on the LAGEOS satellite and considered the impact of the disturbing effect on all the orbital elements (and not only in the eccentricity excitations, orbit inclination and semimajor axis);

(ii) we extended the study to the LAGEOS II satellite;

(iii) we compared the two models (fast-rotation approximation *vs.* slow-rotation one, i.e. the general model) from the epoch of launch of the two satellites up to 2008;

(iv) finally, we compared the impact of the perturbation on the various orbital elements with the residuals of these elements independently obtained with GEODYN.

In the case of the LAGEOS satellite, figure 6, figure 7 and figure 8 show the radial, transversal and out-of-plane components of the perturbing acceleration — in the Gauss co-moving frame with the satellite orbit (see (Milani et al. 1987)) — produced by the Yarkovsky-Schach effect for the two analyzed models: the fast-rotation approximation (red line) and the general model (blue line) for the slow-rotation. The starting epoch is that of the satellite launch, May 14, 1976, and for the spin model we used our new model described in section 6.1.

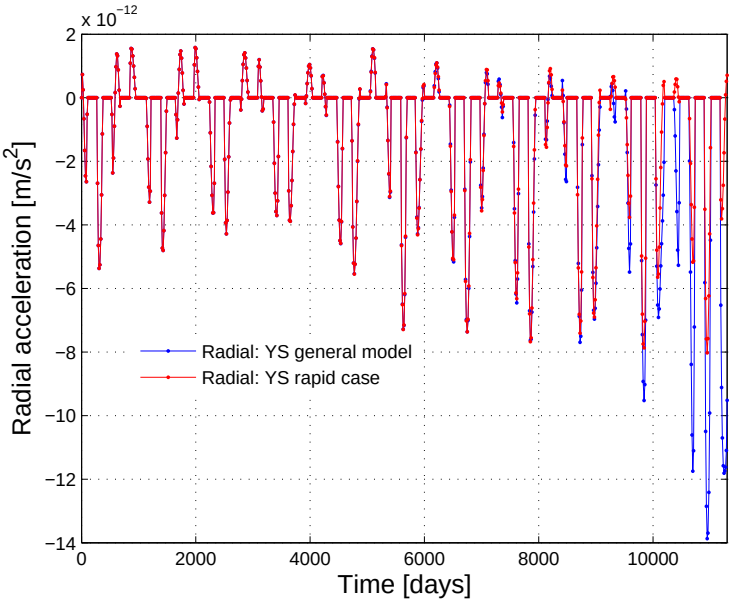

Figure 6. LAGEOS radial acceleration (m/s^2) due to the Yarkovsky-Schach effect perturbation: rapid spin case (red) compared with the general model (blue) developed by (Farinella & Vokrouhlický 1996).

As we can see, the two models give the same predictions for the three accelerations in the Gauss reference frame for a considerable fraction of the analyzed time span. The discrepancy between the two models starts to be apparent after 9000 days, i.e., around the year 2000, that is when the rotational period of LAGEOS was probably of the order of about 2000 s, see Figure 5, close to the lower limit estimated for the thermal inertia of the satellite CCRs. This means that after this epoch the two equatorial components of the thermal thrust acceleration start to produce a non-negligible contribution to the magnitude of the perturbing effect because of the slowing down of the satellite spin rate. Figure 9 shows the impact of the Yarkovsky-Schach perturbation on the rate of LAGEOS argument of perigee over the same time span. Again, as for the components of the perturbing acceleration, after the year 2000 the discrepancy between the two models becomes apparent in the considered element.

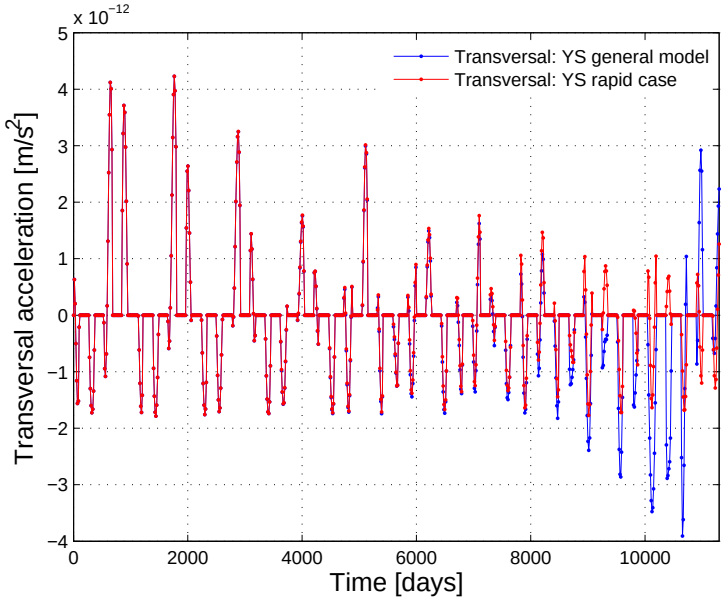

Figure 7. LAGEOS transversal acceleration (m/s^2) due to the Yarkovsky-Schach effect perturbation: rapid spin case (red) compared with the general model (blue) developed by (Farinella & Vokrouhlický 1996).

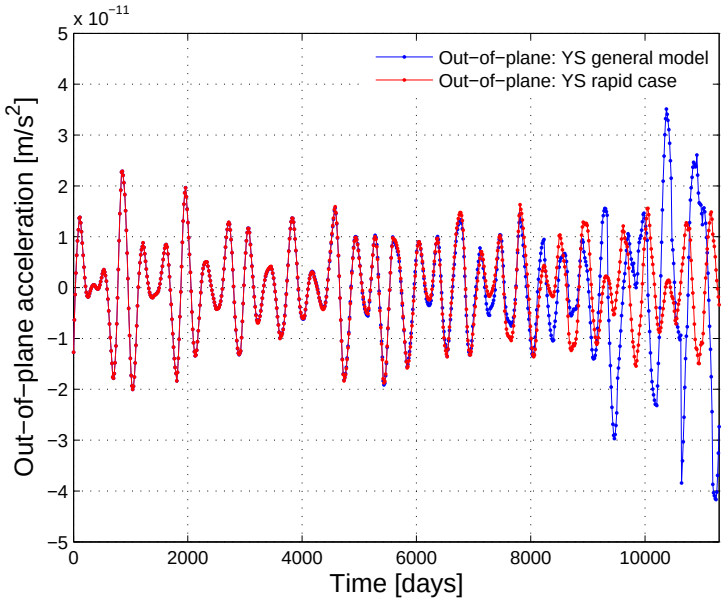

Figure 8. LAGEOS out-of-plane acceleration (m/s^2) due to the Yarkovsky-Schach effect perturbation: rapid spin case (red) compared with the general model (blue) developed by (Farinella & Vokrouhlický 1996).

6.3. Drag forces

The force due to the atmospheric drag represents one of the most difficult to model for a satellite orbiting the Earth, also in case of spherical in shape and passive satellites

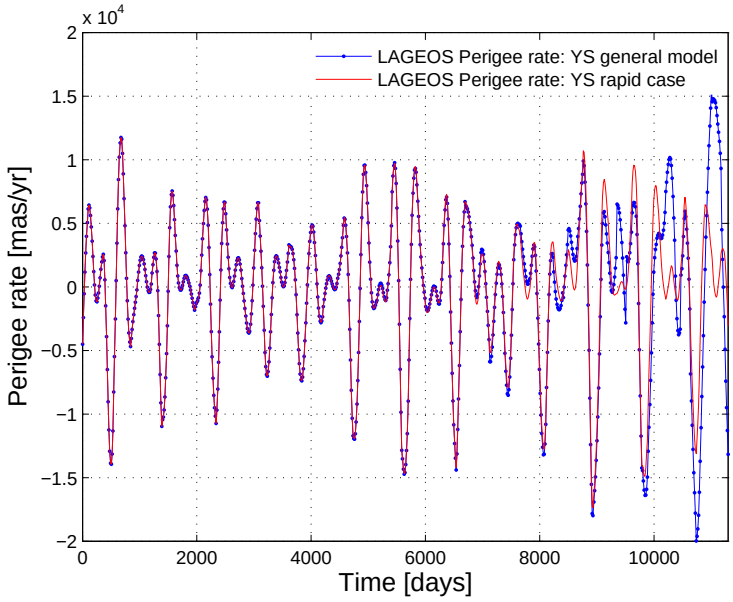

Figure 9. LAGEOS argument of perigee rate (mas/yr) due to the Yarkovsky-Schach effect perturbation: rapid spin case (red) compared with the general model (blue) developed by (Farinella & Vokrouhlický 1996).

such as the two LAGEOS and LARES. The time dependence of the physical properties of the atmosphere and of its main constituents, and the consequent complex interaction between the physical constituents of the satellite surface and the atmosphere ones, are responsible of the modelling difficulties of the drag perturbation. Indeed, the solar and geomagnetic activities play a fundamental role in determining the atmosphere behavior.

The atmosphere constituents may be either neutral particles (as molecular nitrogen N_2, atomic O and molecular O_2 oxygen, helium He, argon Ar and hydrogen H) or charged particles (as ions of hydrogen H^+, helium He^+ and oxygen O^+). Consequently, the interaction may be either in the form of direct collisions with the neutral species and the charged ones (in the case of no charging of the satellite surface), or via a more complex interaction that arises from *Coulomb's* long-range force between the charged surface and the ion species in the satellite surroundings.

Finally, a significant key role is played by the illumination conditions of the satellite surface and their modulation produced by the eclipses. In fact, the illumination conditions influence the local atmosphere temperature and species concentration, as well as the equilibrium potential of the satellite with respect to its environment and, ultimately, the interaction between the satellite and the neutral and charged particles.

In the context of the LARASE experiment, we aim to estimate more accurately the impact of both neutral and charged drag on the orbit of the two LAGEOS satellites and on that of LARES. Obviously, because of its much lower orbit, we expect that this disturbance will have a more profound impact on the orbit of LARES than on those of the two LAGEOS satellites. This aspect is important for future measurements of the

Lense–Thirring effect which involve the use of LARES ascending node as observable.

In the case of the two LAGEOS satellites, the impact of the drag perturbation (neutral plus charged) is masked by larger unmodelled thermal effects, as those due to the Yarkovsky-Schach effect and to the Earth-Yarkovsky effect (this effect, also known as Rubincam effect, is a thermal drag perturbation due to Earth's infrared radiation, and it is responsible of about 70% of the observed decay of the LAGEOS satellites semimajor axis), and by the perturbation provoked by the asymmetric reflectivity of their surface (see (Scharroo et al. 1991, Métris et al. 1997, Lucchesi 2003*b*, Lucchesi 2004*a*)).

Usually, in case of studies and applications in the fields of geophysics and space geodesy, all these unmodelled effects are handled — when possible — by a careful use of empirical accelerations. However, in case of fundamental physics measurements, it is preferable to use only marginally (and still carefully) these empirical accelerations, as in (Ciufolini & Pavlis 2004, Ciufolini et al. 2006), or to entirely avoid their use, as in (Lucchesi & Peron 2010, Lucchesi & Peron 2014).

Therefore, a refinement and an improvement in the modelling of these perturbations — in particular of the thermal models — and their full inclusion in the software used for the POD will allow the possibility to directly highlight the drag effects in the orbital residuals of the considered satellite after the data reduction. This will be of twofold importance: i) a more precise POD will be reached, which will be particularly important in fundamental physics applications; ii) this result will improve, indirectly, the atmospheric models up to an altitude close to 6000 km, by comparing for instance the (extrapolated) predictions of these models for the mean density of the atmosphere with the indirect measurements of this physical quantity that are derived from the final POD.

Indeed, our orbit fit for the two LAGEOS satellites — in terms of the RMS of the range residuals — is at a level of 1-2 cm over 14-day arcs, when the empirical accelerations are used during the orbit fit in order to absorb the unmodelled effects; up to about 10 cm when the empirical accelerations are not used and the thermal effects and the drag effects are not included in the dynamical models (see e.g. (Lucchesi & Peron 2010, Lucchesi & Peron 2014)). This means that the current orbit accuracy is enough to highlight the neutral drag effects (once the thermal effects are modelled) that are responsible — over a 14 days time span — of an along-track displacement of a fraction of a meter.

A great difficulty — that directly impacts on our modelling capabilities — arises from the absence of direct measurements of the atmosphere properties at the relevant altitudes. In fact, the several models developed for the atmosphere, and applied for the studies of Low Earth Orbit (LEO) satellites and satellites re-entry, are characterized by a non-uniform set of measurements (usually obtained with different techniques) up to an altitude of about 1000 km. With regard to the altitudes in the range between 1000 km and 2000 km, these are characterized by an even more sparse set of measurements for the main parameters of the atmosphere. Consequently, we based our analysis of the drag impact on the satellites orbit on extrapolations of these models at about 1450 km

for LARES and at about 5900 km in the case of the two LAGEOS.

In particular, we took advantage of the software SATellite Reentry Analysis Program (SATRAP) (Pardini & Anselmo 1994, Pardini et al. 2012) that is able to load several different models for the Earth's atmosphere together with the appropriate geomagnetic and solar activities indices, while using the following dynamical models for the orbit propagation of the satellite: i) Earth's geopotential, ii) luni-solar perturbations, iii) solar radiation pressure with eclipses and iv) neutral drag.

Therefore, with SATRAP — without prejudice to the above constraints and limitations — we are able to directly investigate the impact of the neutral drag on the satellites orbit using the current best available models for the atmosphere's main constituents. This is also the first step to be performed in order to distinguish the orbital disturbing effects as due to neutral or charged particle drag.

The following activities have been started concerning the impact of the neutral drag perturbations on the satellites orbit:

(i) comparison of the different atmospheric models at the altitudes of interest;

(ii) estimate of the perturbing accelerations in the Mean Of Date (MOD) and Gauss reference systems;

(iii) estimate of the disturbing effects on the orbital elements of the satellites.

Among the many models that SATRAP can include for the modelling of the Earth's atmosphere, in our evaluations we considered the following: the Jacchia-Roberts 1971 (Cappellari et al. 1976), the Mass Spectrometer and Incoherent Scatter 1986 (Hedin 1987), the Mass Spectrometer and Incoherent Scatter Radar Extended 1990 (Hedin 1991), the Naval Research Laboratory MSISE-2000 (Picone et al. 2002), the Empirical Russian model GOST-2004 (Volkov 2004) and, finally, the Jacchia-Bowman 2008 (Bowman et al. 2008).

In figure 10, figure 11 and figure 12 are shown — in the case of the NRLMSISE-2000 model — the neutral drag accelerations (in the Gauss co-moving frame) for LAGEOS as obtained by SATRAP over an 11 years time span, i.e., over an entire solar cycle starting from January 1, 1993.

Such accelerations have been computed also for LAGEOS II and LARES. In table 6 are shown the results for the three components of the accelerations (averaged over the time span of our current analysis: about 4017 days for the two LAGEOS and about 764 days for LARES) of the neutral drag effects for the three satellites. As we can see, despite its smaller value for the area-to-mass ratio, in the case of LARES the accelerations are much larger than those obtained for the two LAGEOS. This is of course due to the higher values for the density at the height of LARES with respect to the density "felt" by the two LAGEOS, at their much higher altitude. Indeed, in figure 13 are shown the density profiles for the three satellites over a common time span, hence under the same conditions for the solar and geomagnetic activities.

As we can see from the results of our simulation, the density at the height and inclination of LARES is on the average about 80 times larger than the (almost equal)

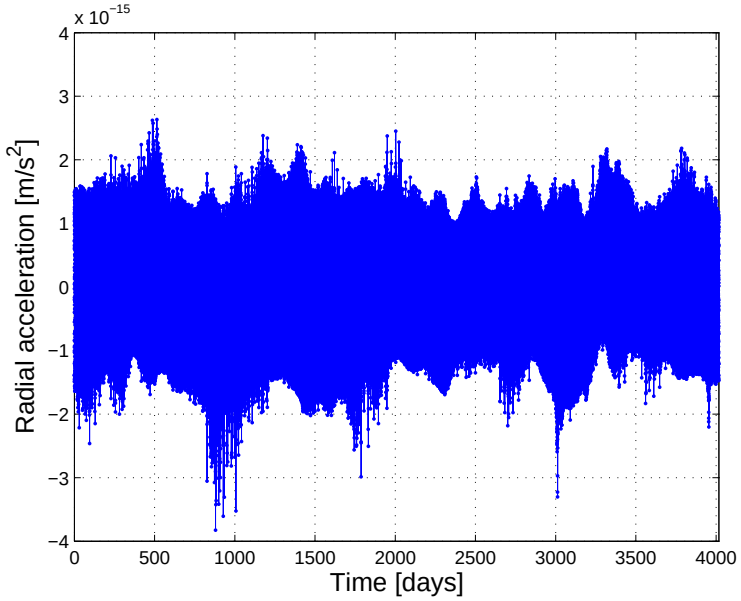

Figure 10. LAGEOS radial acceleration (m/s^2) due to the neutral drag perturbation as obtained from SATRAP over an entire solar cycle using NRLMSISE-2000 to model the Earth's atmosphere.

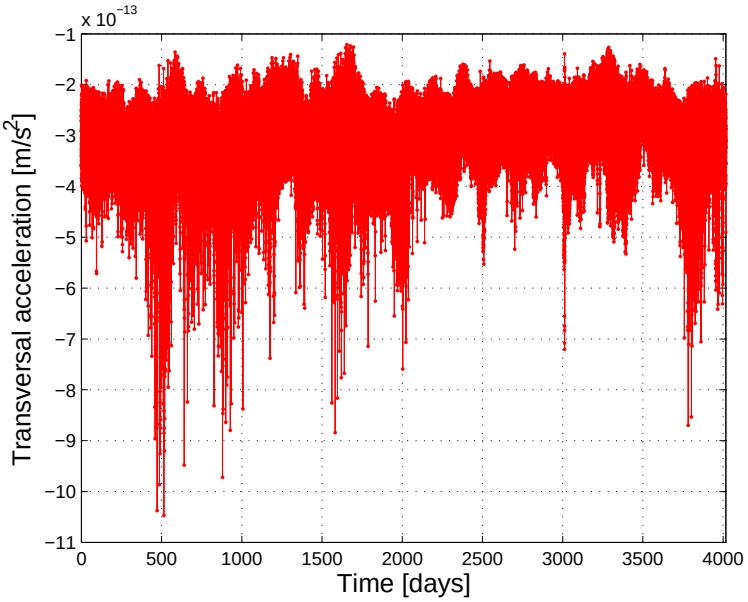

Figure 11. LAGEOS transversal acceleration (m/s^2) due to the neutral drag perturbation as obtained from SATRAP over an entire solar cycle using NRLMSISE-2000 to model the Earth's atmosphere.

density experienced by the two LAGEOS. These results have been obtained applying the NRLMSISE-2000 model for the Earth's atmosphere behavior over the considered time span.

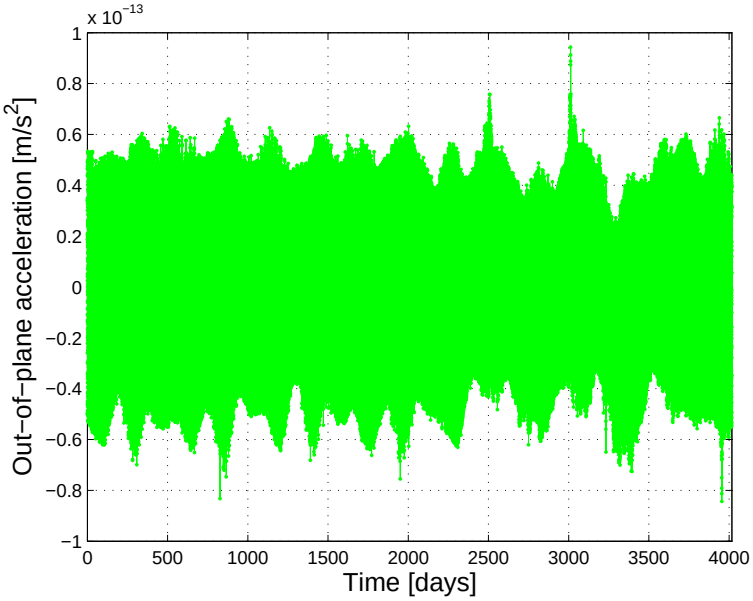

Figure 12. LAGEOS out-of-plane acceleration (m/s^2) due to the neutral drag perturbation as obtained from SATRAP over an entire solar cycle using NRLMSISE-2000 to model the Earth's atmosphere.

Table 6. Average accelerations [m/s^2] in the Gauss reference system for the two LAGEOS and LARES. In the case of the two LAGEOS, the average has been computed over a time span of about 4017 days, starting from January 1, 1993. In the case of LARES, the average has been computed over a time span of about 764 days, starting from March 10, 2012.

Acceleration component	LAGEOS	LAGEOS II	LARES
Radial	9.5×10^{-18}	7.5×10^{-18}	-1.3×10^{-15}
Transversal	-3.1×10^{-13}	-2.6×10^{-13}	-1.3×10^{-11}
Out-of-plane	-1.7×10^{-16}	7.1×10^{-18}	-1.8×10^{-14}

6.4. Tidal perturbation

With regard to the gravitational perturbations acting on the orbit of a satellite around the Earth, not only the static part of the geopotential plays a significant role, but also the periodic variations in the gravitational attraction of the planet on the satellite have to be carefully accounted for. Therefore, both solid and ocean tides due to the combined attraction of the Moon and Sun on our planet (see (Melchior 1978)) have to be modelled in order to reduce as much as possible their impact on the satellite orbit reconstruction, especially in the right ascension of the ascending node Ω and in the argument of pericenter ω because of their relevance for relativistic measurements. Solid tides account for about 90% of the total response to the Moon and Sun tidal disturbing potential and are responsible for the larger tidal effects on the orbit of a satellite.

A convenient way to describe the deformations of the Earth due to tidal effects

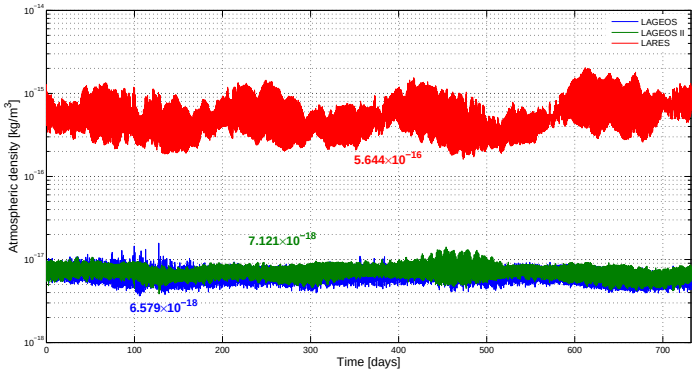

Figure 13. LAGEOS, LAGEOS II and LARES orbit air density [kg/m^3] variation due to the neutral drag as obtained from SATRAP using NRLMSISE-2000 to model the Earth's atmosphere. The time span covers two years since March 10, 2012, a few days after LARES launch. The average densities over the analyzed time span are: $5.6 \cdot 10^{-16}$ kg/m^3, $6.6 \cdot 10^{-18}$ kg/m^3 and $7.1 \cdot 10^{-18}$ kg/m^3, respectively for LARES, LAGEOS and LAGEOS II.

is through the *Love numbers* ($k^f_{2,m} \simeq 0.30$, where f represents the frequency of the tidal wave), which measure the ratio between the response of the real Earth and the theoretical response of a perfect fluid sphere. The Love numbers are determined with high accuracy because of their long–term effects on geodetic satellites, as in the case of the two LAGEOS (see e.g. (Cheng et al. 1997, Wu et al. 2001)). In particular, in the case of solid tides, the degree $\ell = 2$ terms, i.e., those due to the quadrupole tidal potential, are the most important to be considered.

Ocean tides are difficult to be modelled because of the greater complexity of the involved phenomena. Indeed, even if ocean tides account for about 10% only of the total response to the cited external potentials, because of their greater complexity, their uncertainties are a factor of 10 larger than those of solid tides.

Tidal effects are important to be considered because they influence the satellite orbit under three main aspects:

(i) *kinematic effect*: because they produce periodic pulsations of the Earth and, as a consequence, of the on–ground tracking stations;

(ii) *dynamic effect*: because they cause a time variation of the geopotential, that affects the satellite orbit;

(iii) *reference system effect*: because they perturb the Earth rotation, thus affecting the reference systems used in the orbit computation.

In the case of LARES, due to its (much) lower height with respect to that of the two LAGEOS, the perturbation provoked by the tides has a larger impact on its orbit. Therefore, in this case we expect a larger impact of the tides uncertainties on the accuracy of the orbit determination, especially in the case of the ocean tides. Concerning the impact of these uncertainties on the orbit of a satellite, the tidal perturbations

may be divided into two classes: i) those with periods P shorter than the observation period T we consider for the analysis of the relativistic effects, and ii) those with longer periods. The former ones, $P \leq T$, even if not modelled, tend to average out because they perform full cycles or quasi full cycles during the observation period. Conversely, the tides with $P > T$ are more dangerous, because they mimic a pseudo-secular trend that superimposes to the relativistic secular effect to be recovered. However, this last sentence is true if phase and period of the tide are unknown, which is not the case. Indeed, tides with periods longer than the observational time span may be fitted and removed from the residuals if their periods and phases are known.

As part of the activities of LARASE, on one side we reviewed the impact of both solid and ocean tides on the orbit of the two LAGEOS, completing and extending previous studies (see (Bertotti & Carpino 1989, Iorio 2001, Pavlis & Iorio 2002)), and, on the other side, we estimated their impact on the orbit of LARES.

For instance, by using the Lagrange equation for the perturbation of the right ascension of the ascending node, where the perturbing function is given by the potential with which the Earth responds to the tidal perturbations of Moon and Sun, the amplitude of the rate of advance of the nodes of the satellites at a given degree in the expansion of the tidal potential and at a given frequency can be computed:

$$\Delta\Omega_f = \frac{g}{na^2\sqrt{1-e^2}\sin i}\sum_{m=0}^{\ell}\left(\frac{R_\oplus}{a}\right)^{\ell+1} A_{\ell m}\sum_{p=0}^{\ell}\sum_{q=-\infty}^{+\infty}\frac{dF_{\ell mp}}{di}G_{\ell pq}\frac{k_{\ell m}^{(f)}H_\ell^m}{f_I} \tag{49}$$

where

$$g = \frac{GM_\oplus}{R_\oplus^2} \tag{50}$$

and

- ℓ, m: degree and order in the expansion of the tidal potential;
- p, q: auxiliary indices of the expansion of the tidal potential;
- $F_{\ell mp}, G_{\ell mp}$: inclination and eccentricity functions (Kaula,1966);
- $k_{\ell m}^{(f)}$: Love numbers;
- H_ℓ^m: amplitudes in the expansion of the tidal potential.

In table 7 and table 8 are shown the results (amplitude and period) we obtained for a few solid tides in the case of the ascending node of the three satellites. We considered the degree $\ell = 2$ terms, which are the most important to be modelled. In particular, in table 7 are shown the results for the main solid zonal tides ($j_1 = m = 0$), while in table 8 are shown the results we obtained in the case of the main solid tesseral tides ($j_1 = m = 1$). As we can see, in the case of LARES the amplitudes obtained for the angular displacement of the satellite ascending node are larger than those obtained for the two LAGEOS satellites.

In conclusion, considering the values of the amplitudes of the tides shown in table 7, we can state that the uncertainties for the amplitudes of the main solid and ocean tides

Table 7. Impact of the Earth's solid zonal tides ($\ell = 2$ and $m = 0$) on the right ascension of the ascending node Ω of the two LAGEOS and LARES. The periodicities are in days while the amplitudes are in mas. The positive sign (+) of the period refers to westward tidal waves, while the negative sign (−) refers to eastward ones.

Tide	Period	LAGEOS	LAGEOS II	LARES
055.565	6798.38	−1080.22	1976.46	5332.68
055.575	3399.19	−5.23	9.57	25.81
056.554 S_a	365.25	9.97	−18.24	−49.20
057.555 S_{sa}	182.625	31.15	−56.99	−153.75

Table 8. Impact of the Earth's solid tesseral tides ($\ell = 2$ and $m = 1$) on the right ascension of the ascending node Ω of the two LAGEOS and LARES. The periodicities are in days while the amplitudes are in mas. The positive sign (+) of the period refers to westward tidal waves, while the negative sign (−) refers to eastward ones.

Tide	Period	LAGEOS	Period	LAGEOS II	Period	LARES
165.545	1232.95	−40.95	−525.23	7.33	−225.77	35.74
165.555 K_1	1043.67	1738.57	−569.21	−398.25	−223.53	−1853.77
165.565	904.77	202.12	−621.22	−58.29	−241.84	−257.44
163.555 P_1	−221.36	135.76	−138.26	35.62	−102.48	299.51

that influence the long-term evolution of the right ascension of the ascending node of the LARES satellite could impact in a non-negligible way on the recovery of the relativistic precession of the satellite node and, as a consequence, on the precision and accuracy of a new measurement of the Earth's gravitomagnetic field. Conversely, the long-term analysis of the orbit of LARES, in particular of its inclination, eccentricity and node, will help to improve current models for Earth's tides, especially for the ocean ones.

7. Conclusions and recommendations

Einstein's general relativity is today considered as the standard theory for the description of the gravitational interaction, both at low and high energies scales. However, several modern theories of physics — not only new gravitational theories, but also those that aim to include general relativity into the realm of quantum theories — suggest the existence of additional fields in mediating the gravitational interaction to complement the spacetime tensor of general relativity. These fields may have a scalar or vector character, as well as a tensorial one.

Therefore, under the very significant implications that follow from the above considerations, such as the possibility of a violation of the inverse square law and/or of the Einstein Equivalence Principle, new and more refined tests and measurements of gravitation are needed. Of course, it will be extremely important that these new measurements are reliable in terms of precision and accuracy of the results obtained.

The new *experiment* denominated LARASE (LAser RAnged Satellites Experiment), that we have described in the previous sections, aims to contribute to these new measurements of relativistic gravity in the WFSM limit of general relativity. In particular, we have described the main measurements to be performed in the future, with the state of the art of their results and constraints in term of precision and accuracy.

The test masses of the LARASE experiment are passive satellites tracked by the ILRS network, in particular the two LAGEOS and the new LARES. Therefore, in order to reach a precise orbit determination for these satellites, it is necessary to develop, for each of them, dynamical models able to take into account very small effects, such as those predicted by Einstein's geometrodynamics, and also as small as those that the powerful SLR technique allows to measure.

In this context, within LARASE we started an activity to review previous models developed for the two LAGEOS, in particular those related to the non-conservative forces. This activity is also very important in the case of LARES. In particular, we must verify how well the previous models can be applied to LARES, what new aspects, if any, are to be considered, and whether new dedicated models need to be built up.

In previous sections, we focused on some of the activities we started and we also provided some new results. We went back to the thermal effects on the two LAGEOS, and in particular we focused on the transition from the fast spin approximation to the slow spin one in the case of the Yarkovsky–Schach effect. Regarding this issue, we deeply reviewed previous models for the spin axis evolution of the satellites and we highlighted some of our results for LAGEOS in the rapid spin case. Moreover, we have removed all the semplifying hypotheses at the basis of previous models and we have found a general solution not restricted to averaged equations for the various torques involved.

Another issue that we analyzed, still dealing with the modelling of the non-gravitational perturbations, has been the neutral drag acceleration, particularly important for LARES due to its lower altitude with respect to that of the two LAGEOS. Indeed, beside the use of GEODYN, which is our reference software for the data reduction of the SLR NP and, consequently, for the POD of the satellites, we used a dedicated software (SATRAP) which is able to easily handle the various atmospheric models developed by the research community which is involved in this field. We have computed, for the various atmospheric models, the neutral drag accelerations in the Gauss frame and we compared the results so obtained. We also determined the long-term effects of the various models on the orbit of the satellites and, despite the small value for the area-to-mass ratio of LARES, we have seen that the drag effect has a significant impact on the orbit of the satellite.

Finally, we started an activity for reviewing the gravitational dynamic models and the estimate of the main systematic errors associated with them. We have shown some of our results on the impact of the Earth's solid tides on the nodes of the considered satellites. Again, in the case of LARES the effects are significant because of its small height. This will constitute a significant issue, to be carefully considered in the perspective of future relativistic measurements with LARES, in particular for the

ocean tides, which are characterized by much larger uncertainties with respect to those of the solid tides. This work on tides revisits and extends the previous studies of the tidal effects on the orbit of the two LAGEOS.

Concluding, with LARASE we want to provide new and refined measurements of gravitation in the field of the Earth. These measurements should be reliable, i.e., they should be unassailable concerning their precision and the estimate of their systematic uncertainties. This objective can be achieved only through a significant revision of existing dynamical models for the description of the orbit of the satellites and the consequent development of new and more accurate models, especially for non-gravitational forces. This activity is ongoing.

Acknowledgments

The authors acknowledge the ILRS for providing high quality laser ranging data of the two LAGEOS satellites and of LARES. Special thanks for helpful comments to G. Bianco (ASI/CGS, Matera, Italy) and to V. Luceri (e-GEOS, ASI/CGS, Matera, Italy). We are also grateful to S. Pirrotta (ASI, Roma) and E. Flamini (ASI, Roma) for providing a few documents on the LARES satellite and to C. Portelli (ASI, Roma) and P. Messidoro (Thales, Torino, Italy) for a document on the LAGEOS II satellite. This work has been in part supported by the Commissione Scientifica Nazionale II (CSNII) on astroparticle physics experiments of the italian Istituto Nazionale di Fisica Nucleare (INFN). In this regard, we would like to thank Prof. R. Battiston (president of ASI, Roma, Italy) as the former president of CSNII for having supported the LARASE program within the experiments of the astroparticle commission of INFN. Finally, we thank two anonymous reviewers for their helpful comments and suggestions.

References

Adelberger E G, Heckel B R & Nelson A E 2003 *Annu. Rev. Nucl. Part. Sci.* **53**, 77–121.

Adhikari R X 2014 *Rev. Mod. Phys.* **86**, 121–151.
*http://link.aps.org/doi/10.1103/RevModPhys.86.121

Afonso G, Barlier F, Mignard F, Carpino M & Farinella P 1989 *Ann. Geophysicae* **7**, 501–514.

Altamimi Z, Collilieux X & Métivier L 2011 *J. Geod.* **85**, 457–473.

Andrés de la Fuente J I 2007 Enhanced Modelling of LAGEOS Non-Gravitational Perturbations PhD thesis Delft University Press Sieca Repro, Turbineweg 20, 2627 BP Delft, The Netherlands.

Andrés J I, Noomen R, Bianco G, Currie D G & Otsubo T 2004 *J. Geophys. Res.* **109**, 6403.

Ashby N & Bertotti B 1984 *Phys. Rev. Lett.* **52**, 485–488.

Ashby N & Bertotti B 1986 *Phys. Rev. D* **34**, 2246–2259.

Astone P, Baggio L, Bassan M, Bignotto M, Bonaldi M, Bonifazi P, Cavallari G, Cerdonio M, Coccia E, Conti L, D'Antonio S, di Paolo Emilio M, Drago M, Fafone V, Falferi P, Foffa S, Fortini P, Frasca S, Giordano G, Hamilton W O, Hanson J, Johnson W W, Liguori N, Longo S, Maggiore M, Marin F, Marini A, McHugh M P, Mezzena R, Miller P, Minenkov Y, Mion A, Modestino G, Moleti A, Nettles D, Ortolan A, Pallottino G V, Pizzella G, Poggi S, Prodi G A, Re V, Rocchi A, Ronga F, Salemi F, Sturani R, Taffarello L, Terenzi R,

Vedovato G, Vinante A, Visco M, Vitale S, Weaver J, Zendri J P & Zhang P 2010 *Phys. Rev. D* **82**, 022003.
*http://link.aps.org/doi/10.1103/PhysRevD.82.022003

Avizonis J P V 1997 Remote Sensing of the Lageos-I Spin-Axis and Image Processing for Advanced Optical Systems PhD thesis UNIVERSITY OF MARYLAND COLLEGE PARK.

Baeßler S, Heckel B R, Adelberger E G, Gundlach J H, Schmidt U & Swanson H E 1999 *Phys. Rev. Lett.* **83**, 3585–3588.

Bennett C L, Halpern M, Hinshaw G, Jarosik N, Kogut A, Limon M, Meyer S S, Page L, Spergel D N, Tucker G S, Wollack E, Wright E L, Barnes C, Greason M R, Hill R S, Komatsu E, Nolta M R, Odegard N, Peiris H V, Verde L & Weiland J L 2003 *Astrophys. J. Suppl.* **148**, 1–27.

Bertotti B & Carpino M 1989 Supplementary satellites and tidal perturbations in Measurement of the Gravitomagnetic Field Using a Pair of Laser Ranged Satellites Technical report.

Bertotti B & Iess L 1991 *J. Geophys. Res.* **96**, 2431–2440.

Bertotti B, Iess L & Tortora P 2003 *Nature* **425**, 374–376.

Beutler G, Drinkwater M R, Rummel R & von Steiger R, eds 2003.

Bizouard M A 2014 *General Relativity and Gravitation* **46**, 1763.

Bolton C T 1972 *Nature* **235**, 271–273.

Bowman B R, Tobiska W K, Marcos F A, Huang C Y, Lin C S & Burke W J 2008 *in* 'AIAA/AAS Astrodynamics Specialist Conference, 18-21 August 2008, Honolulu, Hawaii' number AIAA 2008-6438.

Brans C & Dicke R H 1961 *Phys. Rev.* **124**, 925–935.

Cappellari J O, Velez C E & Fuchs A J 1976 *NASA STI/Recon Technical Report N* **76**, 24291.

Chashchina O I, Iorio L & Silagadze Z K 2009 *Acta Phys.Polon.* **B40**, 2363–2378.

Cheng M K, Shum C K & Tapley B D 1997 *J. Geophys. Res.* **102**, 22377.

Ciufolini I 1984 Theory and experiments in General Relativity and other metric theories PhD thesis Univ. of Texas, Austin Pub. Ann. Arbor. Michigan.

Ciufolini I 1986 *Phys. Rev. Lett.* **56**, 278–281.

Ciufolini I 1989 *Int. J. Mod. Phys. A* **4**, 3083–3145.

Ciufolini I 1996 *Nuovo Cim. A* **109**, 1709–1720.

Ciufolini I, Chieppa F, Lucchesi D & Vespe F 1997 *Class. Quantum Grav.* **14**, 2701–2726.

Ciufolini I, Lucchesi D, Vespe F & Chieppa F 1997 *Europhys. Lett.* **39**, 359–364.

Ciufolini I, Lucchesi D, Vespe F & Mandiello A 1996 *Nuovo Cim. A* **109**, 575–590.

Ciufolini I & Matzner R 1992 *Int. J. Mod. Phys. A* **7**, 843–852.

Ciufolini I, Paolozzi A, Pavlis E C, Ries J C, Koenig R, Matzner R A, Sindoni G & Neumayer H 2009 *Space Sci. Rev.* **148**, 71–104.

Ciufolini I & Pavlis E C 2004 *Nature* **431**, 958–960.

Ciufolini I, Pavlis E C & Peron R 2006 *New Astron.* **11**, 527–550.

Ciufolini I, Pavlis E, Chieppa F, Fernandes-Vieira E & Perez-Mercader J 1998 *Science* **279**, 2100–2103.

Ciufolini I & Wheeler J A 1995 *Gravitation and inertia* Princeton University Press Princeton.

Cohen S C, King R W, Kolenkiewicz R, Rosen R D & Schutz B E 1985 *J. Geophys. Res.* **90**, 9215–9438.

Cugusi L & Proverbio E 1978 *Astron. Astrophys.* **69**, 321–325.

Damour T 1996 *Class. Quantum Grav.* **13**, A33–A41.

Damour T & Esposito-Farèse G 1994 *Phys. Rev. D* **49**, 1693–1706.

Damour T, Piazza F & Veneziano G 2002*a* *Phys. Rev. Lett.* **89**(8), 081601.

Damour T, Piazza F & Veneziano G 2002*b* *Phys. Rev. D* **66**, 046007.

Damour T & Polyakov A M 1994 *Nucl. Phys. B* **423**, 532–558.

Damour T, Soffel M & Xu C 1991 *Phys. Rev. D* **43**, 3273–3307.

Damour T, Soffel M & Xu C 1992 *Phys. Rev. D* **45**, 1017–1044.

Damour T, Soffel M & Xu C 1993 *Phys. Rev. D* **47**, 3124–3135.
Damour T, Soffel M & Xu C 1994 *Phys. Rev. D* **49**, 618–635.
de Sitter W 1916 *Mon. Not. R. Astron. Soc.* **77**, 155–184.
Degnan J J 1985 *IEEE Trans. Geosci. Remote Sensing* **23**, 398–413.
Dicke R H 1962 *Phys. Rev.* **125**, 2163–2167.
Dicke R H 1964 *The Theoretical Significance of Experimental Relativity* Blackie and Son Ltd. London and Glasgow.
Dicke R H 1968 *Astrophys. J.* **152**, 1.
Einstein A 1908 *Jahrbuch der Radioaktivität und Elektronik* **4**, 411–462.
Einstein A 1915 *Sitzungsber. preuss.Akad. Wiss., vol. 47, No.2, pp. 831-839, 1915* **47**, 831–839.
Einstein A 1916 *Annalen der Physik* **354**, 769–822.
Everitt C W F, Debra D B, Parkinson B W, Turneaure J P, Conklin J W, Heifetz M I, Keiser G M, Silbergleit A S, Holmes T, Kolodziejczak J, Al-Meshari M, Mester J C, Muhlfelder B, Solomonik V G, Stahl K, Worden, Jr. P W, Bencze W, Buchman S, Clarke B, Al-Jadaan A, Al-Jibreen H, Li J, Lipa J A, Lockhart J M, Al-Suwaidan B, Taber M & Wang S 2011 *Physical Review Letters* **106**(22), 221101.
Farinella P, Nobili A M, Barlier F & Mignard F 1990 *Astron. Astrophys.* **234**, 546–554.
Farinella P & Vokrouhlický D 1996 *Plan. Space Sci.* **44**, 1551–1561.
Farinella P, Vokrouhlicky D & Barlier F 1996 *J. Geophys. Res.* **101**, 17861–17872.
Fienga A, Laskar J, Kuchynka P, Leponcin-Lafitte C, Manche H & Gastineau M 2009 *in* 'Relativity in Fundamental Astronomy: Dynamics, Reference Frames, and Data Analysis' Vol. 5 of *Proceedings of the International Astronomical Union* pp. 159–169.
*http://journals.cambridge.org/article$_S$1743921309990330
Fischbach E & et al. 1986 *Phys. Rev. Lett.* **56**, 3–6.
Habib S, Holz D E, Kheyfets A, Matzner R A, Miller W A & Tolman B W 1994 *Phys. Rev. D* **50**, 6068–6079.
Hammond R T 2002 *Rep. Prog. Phys.* **65**, 599–649.
Hedin A E 1987 *J. Geophys. Res.* **92**, 4649–4662.
Hedin A E 1991 *J. Geophys. Res.* **96**, 1159–1172.
Hehl F W, von der Heyde P, Kerlick G D & Nester J M 1976 *Rev. Mod. Phys.* **48**, 393–416.
Hewish A, Bell S J, Pilkington J D H, Scott P F & Collins R A 1968 *Nature* **217**, 709–713.
Huang C, Ries J C, Tapley B D & Watkins M M 1990 *Celest. Mech. Dyn. Astron.* **48**, 167–185.
Hulse R A & Taylor J H 1975 *Astrophys. J.* **195**, L51–L53.
International Earth Rotation Service n.d. EOP Combined Series EOP C04 Technical report IERS.
Iorio L 2001 *Celest. Mech. Dyn. Astron.* **79**, 201–230.
Iorio L, Ciufolini I & Pavlis E C 2002 *Class. Quantum Grav.* **19**, 4301–4309.
Iorio L & Morea A 2004 *Gen. Relativ. Gravit.* **36**, 1321–1333.
Jordan P 1949 *Nature* **164**, 637–640.
Kaula W M 1966 *Theory of satellite geodesy. Applications of satellites to geodesy* Blaisdell Waltham, Mass.
Kerr R P 1963 *Phys. Rev. Lett.* **11**, 237–238.
*http://link.aps.org/doi/10.1103/PhysRevLett.11.237
Koenig R, Moreno Monge B & Michalak G 2012 'Some aspects and perspectives of measuring Lense-Thirring with GNSS and geodetic satellites'.
Kramer M, Stairs I H, Manchester R N, McLaughlin M A, Lyne A G, Ferdman R D, Burgay M, Lorimer D R, Possenti A, D'Amico N, Sarkissian J M, Hobbs G B, Reynolds J E, Freire P C C & Camilo F 2006 *Science* **314**, 97–102.
Kucharski D, Lim H C, Kirchner G & Hwang J Y 2013 *Adv.Space Res.* **52**, 1332–1338.
Kucharski D, Otsubo T, Kirchner G & Bianco G 2012 *Adv.Space Res.* **50**, 1473–1477.
Landau L D & Lifshitz E M 1960 *Electrodynamics of continuous media*.
Lemoine F G & et al. 1998 The Development of the Joint NASA GSFC and the National Imagery

and Mapping Agency (NIMA) Geopotential Model EGM96 Technical Paper NASA/TP–1998–206861.

Lense J & Thirring H 1918 *Phys. Z.* **19**, 156.

Lerch F J, Klosko S M, Patel G B & Wagner C A 1985 *J. Geophys. Res.* **90**, 9301–9311.

Lerch F J, Klosko S M, Wagner C A & Patel G B 1985 *J. Geophys. Res.* **90**, 9312–9334.

Li G & Zhao H 2005 *Int. J. Mod. Phys. D* **14**, 1657–1666.

Lucchesi D 2001 Effets the Forces non-gravitationnelles sur les Satellites LAGEOS: Impact sur la Determination de l'Effet Lense–Thirring PhD thesis Nice-Sophia-Antipolis University, France. Presented at OCA/CERGA Observatory, Grasse, France, December 18, 2001.

Lucchesi D M 2002 *Plan. Space Sci.* **50**, 1067–1100.

Lucchesi D M 2003*a* *Phys. Lett. A* **318**, 234–240.

Lucchesi D M 2003*b* *Geophys. Res. Lett.* **30**, 1957.

Lucchesi D M 2004*a* *Celest. Mech. Dyn. Astron.* **88**, 269–291.

Lucchesi D M 2004*b* *in* J.-P Paillé, ed., '35th COSPAR Scientific Assembly' Vol. 35 of *COSPAR Meeting* p. 232.

Lucchesi D M 2007 *Adv. Space Res.* **39**, 324–332.

Lucchesi D M 2011 *Adv. Space Res.* **47**, 1232–1237.

Lucchesi D M & Balmino G 2006 *Plan. Space Sci.* **54**, 581–593.

Lucchesi D M, Ciufolini I, Andrés J I, Pavlis E C, Peron R, Noomen R & Currie D G 2004 *Plan. Space Sci.* **52**, 699–710.

Lucchesi D M & Peron R 2006 *in* '36th COSPAR Scientific Assembly' Vol. 36 of *COSPAR Meeting* p. 3228.

Lucchesi D M & Peron R 2010 *Phys. Rev. Lett.* **105**(23), 231103.

Lucchesi D M & Peron R 2014 *Phys. Rev. D* **89**(8), 082002.

Mao Y, Tegmark M, Guth A H & Cabi S 2007 *Phys. Rev. D* **76**(10), 104029.

March R, Bellettini G, Tauraso R & Dell'Agnello S 2011*a* *Gen. Relativ. Gravit.* **43**, 3099–3126.

March R, Bellettini G, Tauraso R & Dell'Agnello S 2011*b* *Phys. Rev. D* **83**(10), 104008.

Marsh J G, Lerch F J, Putney B H, Christodoulidis D C & Smith D E 1988 *J. Geophys. Res.* **93**, 6169–6215.

Mashhoon B, Gronwald F & Lichtenegger H 2001 *in* C Lmmerzahl, C Everitt & F Hehl, eds, 'Gyros, Clocks, Interferometers...: Testing Relativistic Graviy in Space' Vol. 562 of *Lecture Notes in Physics* Springer Berlin Heidelberg pp. 83–108.
*http://dx.doi.org/10.1007/3-540-40988-2_5

Mashhoon B, Hehl F W & Theiss D S 1984 *Gen. Rel. Grav.* **16**, 711–750.

Melchior P 1978 *The tides of the planet earth.*

Métris G, Vokrouhlický D, Ries J C & Eanes R J 1997 *J. Geophys. Res.* **102**, 2711–2729.

Métris G, Vokrouhlický D, Ries J C & Eanes R J 1999 *Adv. Space Res.* **23**, 721–725.

Milani A & Gronchi G 2009 *Theory of Orbit Determination.*

Milani A, Nobili A M & Farinella P 1987 *Non-gravitational perturbations and satellite geodesy* Adam Hilger Bristol.

Misner C W, Thorne K S & Wheeler J A 1973 *Gravitation.*

Moffat J W 1979 *Phys. Rev. D* **19**, 3554–3558.

Moffat J W & Woolgar E 1988 *Phys. Rev. D* **37**, 918–930.

Montenbruck O & Gill E 2000 *Satellite Orbits. Models, Methods and Applications* Springer Berlin.

Müller J, Williams J G & Turyshev S G 2008 *in* H. Dittus, C. Lammerzahl, & S. G. Turyshev, ed., 'Lasers, Clocks and Drag-Free Control: Exploration of Relativistic Gravity in Space' pp. 457–472.

Murphy T W 2013 *Rep. Prog. Phys.* **76**(7), 076901.

Ni W T 1973 *Phys. Rev. D* **7**, 2880–2883.

Nobili A M, Comandi G L, Bramanti D, Doravari S, Lucchesi D M & Maccarrone F 2008 *Gen. Relativ. Gravit.* **40**, 1533–1554.

Nobili A M, Shao M, Pegna R, Zavattini G, Turyshev S G, Lucchesi D M, De Michele A, Doravari S, Comandi G L, Saravanan T R, Palmonari F, Catastini G & Anselmi A 2012 *Class. Quantum Grav.* **29**(18), 184011.

Nordtvedt J K & Will C M 1972 *Astrophys. J.* **177**, 775–792.

Nordtvedt K 1968 *Phys. Rev.* **169**, 1017–1025.

Nordtvedt K 1998 pp. 34–37.

Nordtvedt K 1999 *Classical and Quantum Gravity* **16**, L19–L21.

Nordtvedt K 2000 *Phys. Rev. D* **61**, 122001.

Nordtvedt K 2001 *Surv. Geophys.* **22**, 597–602.

Paolozzi A & Ciufolini I 2013 *Acta Astronautica* **91**, 313–321.

Pardini C & Anselmo L 1994 SATRAP: Satellite reentry analysis program Internal Report C94-17 CNUCE Institute, Consiglio Nazionale delle Ricerche (CNR) Pisa, Italy.

Pardini C, Moe K & Anselmo L 2012 *Plan. Space Sci.* **67**, 130–146.

Pavlis D E & et al. 1998 *GEODYN II Operations Manual* NASA GSFC.

Pavlis E C & Iorio L 2002 *Int. J. Mod. Phys. D* **11**, 599–618.

Pearlman M R, Degnan J J & Bosworth J M 2002 *Adv. Space Res.* **30**, 135–143.

Penrose R 1965 *Phys. Rev. Lett.* **14**, 57–59.

Penzias A A & Wilson R W 1965 *Astrophys. J.* **142**, 419–421.

Peron R 2013 *Mon. Not. R. Astron. Soc.* **432**, 2591–2595.

Petit G & Luzum B 2010 IERS Conventions (2010) IERS Technical Note 36 IERS Frankfurt am Main: Verlag des Bundesamts für Kartographie und Geodäsie.

Picone J M, Hedin A E, Drob D P & Aikin A C 2002 *J. Geophys. Res.* **107**, 1468.

Pitjeva E V 2009 *in* 'IAU Symposium #261, American Astronomical Society' Vol. 261 p. 603.

Poisson E & Will C M 2014 *Gravity.*

Putney B, Kolenkiewicz R, Smith D, Dunn P & Torrence M H 1990 *Adv. Space Res.* **10**, 197–203.

Ray R D 1999 A Global Ocean Tide Model From TOPEX/POSEIDON Altimetry: GOT99.2 Technical Paper NASA/TM-1999-209478 Goddard Space Flight Center, Greenbelt, Maryland.

Reigber C, Lühr H & Schwintzer P 2002 *Adv. Space Res.* **30**, 129–134.

Reigber C, Schmidt R, Flechtner F, König R, Meyer U, Neumayer K H, Schwintzer P & Zhu S Y 2005 *J. Geodyn.* **39**, 1–10.

Reigber C, Schwintzer P, Neumayer K H, Barthelmes F, König R, Förste C, Balmino G, Biancale R, Lemoine J M, Loyer S, Bruinsma S, Perosanz F & Fayard T 2003 *Adv. Space Res.* **31**, 1883–1888.

Ries J C & Eanes R J 2012 *in* 'American Astronomical Society Meeting Abstracts #219' Vol. 219 of *American Astronomical Society Meeting Abstracts* p. 122.04.

Ries J, Eanes R & Tapley B 2003 World Scientific Publishing chapter Lense-Thirring precession determination from laser ranging to artificial satellites, pp. 201–211.

Ries J, Eanes R & Watkins M 2008 *in* '16th International Workshop on Laser Ranging' p. 19.

Riess A G, Filippenko A V, Challis P, Clocchiatti A, Diercks A, Garnavich P M, Gilliland R L, Hogan C J, Jha S, Kirshner R P, Leibundgut B, Phillips M M, Reiss D, Schmidt B P, Schommer R A, Smith R C, Spyromilio J, Stubbs C, Suntzeff N B & Tonry J 1998 *Astron. J.* **116**, 1009–1038.

Rosen N 1973 *Gen. Relativ. Gravit.* **4**, 435–447.

Rosen N 1978 *Gen. Relativ. Gravit.* **9**, 339–351.

Rubincam D P 1977 *Celest. Mech.* **15**, 21–33.

Rubincam D P 1987 *J .Geophys. Res.* **92**, 1287–1294.

Rubincam D P 1988 *J. Geophys. Res.* **93**, 13805–13810.

Rubincam D P 1990 *J. Geophys. Res.* **95**, 4881–4886.

Rubincam D P, Currie D G & Robbins J W 1997 *J. Geophys. Res.* **102**, 585–590.

Rubincam D P, Knocke P, Taylor V R & Blackwell S 1987 *J. Geophys. Res.* **92**, 11662–11668.

Ruhl J E, Ade P A R, Bock J J, Bond J R, Borrill J, Boscaleri A, Contaldi C R, Crill B P, de Bernardis P, De Troia G, Ganga K, Giacometti M, Hivon E, Hristov V V, Iacoangeli A, Jaffe A H, Jones W C, Lange A E, Masi S, Mason P, Mauskopf P D, Melchiorri A, Montroy T, Netterfield C B, Pascale E, Piacentini F, Pogosyan D, Polenta G, Prunet S & Romeo G 2003 *Astrophys. J.* **599**, 786–805.

Scharroo R, Wakker K F, Ambrosius B A C & Noomen R 1991 *J. Geophys. Res.* **96**, 729–740.

Schiff L I 1960 *Physical Review Letters* **4**, 215–217.

Schlamminger S, Choi K Y, Wagner T A, Gundlach J H & Adelberger E G 2008 *Phys. Rev. Lett.* **100**(4), 041101.

Schmidt M 1963 *Nature* **197**, 1040.

Schwartz H M 1977 *Am. J. Phys.* **45**, 899–902.

Shapiro I I 1990 *in* N. Ashby, D. F. Bartlett, & W. Wyss, ed., 'General Relativity and Gravitation, 1989' p. 313.

Shapiro I I, Pettengill G H, Ash M E, Ingalls R P, Campbell D B & Dyce R B 1972 *Phys. Rev. Lett.* **28**, 1594–1597.

Sinclair A T 1997 'Data Screening and Normal Point Formation — Re–Statement of Herstmonceux Normal Point Recommendation'.
*http://ilrs.gsfc.nasa.gov/products$_f ormats_p rocedures/normal_p oint/np_a lgo.html$

Slabinski V J 1996 *Celest. Mech. Dyn. Astron.* **66**, 131–179.

Soffel M H 1989 *Relativity in Astrometry, Celestial Mechanics and Geodesy.*

Soffel M, Klioner S A, Petit G, Wolf P, Kopeikin S M, Bretagnon P, Brumberg V A, Capitaine N, Damour T, Fukushima T, Guinot B, Huang T Y, Lindegren L, Ma C, Nordtvedt K, Ries J C, Seidelmann P K, Vokrouhlický D, Will C M & Xu C 2003 *Astron. J.* **126**, 2687–2706.

Standish E M, Newhall X X, Williams J G & Folkner W M 1995 JPL Planetary and Lunar Ephemerides, DE403/LE403 Technical Report JPL IOM 314.10-127.

Sullivan L J 1980 *in* T. S Hartwick, ed., 'CO2 laser devices and applications' Vol. 227 of *Society of Photo-Optical Instrumentation Engineers (SPIE) Conference Series* pp. 148–161.

Tapley B D & Reigber C 2001 *AGU Fall Meeting Abstracts* p. C2.

Tapley B D, Ries J C, Eanes R J & Watkins M M 1989 Measuring the Lense-Thirring precession using a second LAGEOS satellite Technical Report CSR-89-3 CSR-UT.

Tapley B D, Watkins M M, Ries J C, Davis G W, Eanes R J, Poole S R, Rim H J, Schutz B E, Shum C K, Nerem R S, Lerch F J, Marshall J A, Klosko S M, Pavlis N K & Williamson R G 1996 *J. Geophys. Res.* **101**, 28029.

Tapley B, Schutz B & Born G 2004 *Statistical Orbit Determination* Elsevier Academic Press.
*http://books.google.it/books?id=H-dQhMQohsIC

Touboul P, Métris G, Lebat V & Robert A 2012 *Class. Quantum Grav.* **29**(18), 184010.

Touboul P, Willemenot E, Foulon B & Josselin V 1999 *Boll. Geof. Teor. Appl.* **40**, 321–327.

van Patten R A & Everitt C W F 1976 *Phys. Rev. Lett.* **36**, 629–632.

Veneziano G 1968 *Nuovo Cimento A Serie* **57**, 190–197.

Vokrouhlický D 1996 *Geophys. Res. Lett.* **23**, 3079–3082.

Vokrouhlický D & Métris G 1998 *in* N Capitaine, ed., 'Journées 1997 - Systèmes de Référence Spatio-Temporels' pp. 46–50.

Volkov I I 2004 Earth's upper atmosphere density model for ballistic support of the flight of artificial Earth satellites GOST R 25645.166-2004 Technical report Publishing House of the Standards Moscow.

Weinberg S 1972 *Gravitation and Cosmology: Principles and Applications of the General Theory of Relativity.*

Wheeler J 1964 Gordon and Breach Publishers, Inc.

Will C M 1971 *Astrophys. J.* **163**, 611–628.

Will C M 1993 *Theory and Experiment in Gravitational Physics* Cambridge University Press Cambridge, UK.

Will C M 2011 *Proceedings of the National Academy of Science* **108**, 5938–5945.
Will C M 2014 *Living Rev. Relativity* **17**, 4.
Will C M & Nordtvedt J K 1972 *Astrophys. J.* **177**, 757–774.
Williams J G, Turyshev S G & Boggs D H 2012 *Class. Quantum Grav.* **29**(18), 184004.
Williams S E 2002 The Lageos Satellite: A Comprehensive Spin Model and Analysis PhD thesis NCSU PhD Dissertation, pp. i-xii, 1-252, 2002.
Witten E 1995 *Nuclear Physics B* **443**, 85–126.
Wu B, Bibo P, Zhu Y & Hsu H 2001 *J. Geodetic Soc. Japan* **47**, 174–180.
Yilmaz H 1959 *Bull. Am. Phys. Soc.* **4**, 65.